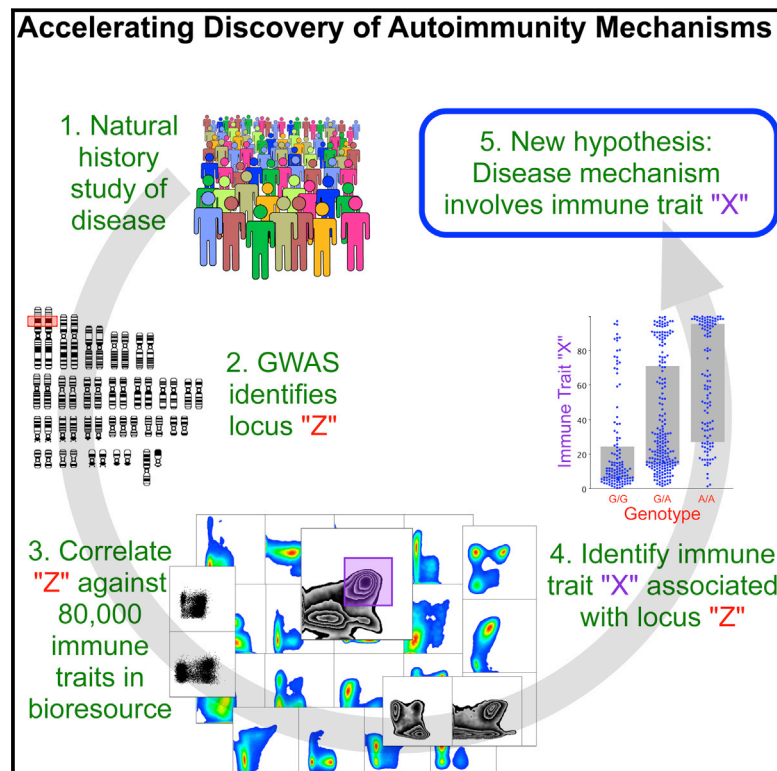


# The Genetic Architecture of the Human Immune System: A Bioresource for Autoimmunity and Disease Pathogenesis

## Graphical Abstract



## Authors

Mario Roederer, Lydia Quaye, ...,  
Tim D. Spector, Frank O. Nestle

## Correspondence

roederer@nih.gov (M.R.),  
tim.spector@kcl.ac.uk (T.D.S.)

## In Brief

The study of a large and homogenous population of human twins identifies numerous genetic loci controlling the phenotype or number of functionally important immune subsets in the blood, providing a database to test associations of any genetic locus with more than 78,000 different immune traits.

## Highlights

- Resource of heritabilities and genetic associations of 80,000 immune traits in 669 twins
- Genetic associations with immune cell frequencies and surface protein expression levels
- Of the top 150 traits, 11 genetic loci explained up to 36% of variation of 19 traits
- Loci include autoimmune susceptibility genes, providing etiological hypotheses



# The Genetic Architecture of the Human Immune System: A Bioresource for Autoimmunity and Disease Pathogenesis

Mario Roederer,<sup>1,7,\*</sup> Lydia Quaye,<sup>2,7</sup> Massimo Mangino,<sup>2,4,7</sup> Margaret H. Beddall,<sup>1</sup> Yolanda Mahnke,<sup>1,5</sup> Pratip Chattopadhyay,<sup>1</sup> Isabella Tosi,<sup>3,4</sup> Luca Napolitano,<sup>3</sup> Manuela Terranova Barberio,<sup>3</sup> Cristina Menni,<sup>2</sup> Federica Villanova,<sup>3,4</sup> Paola Di Meglio,<sup>3,6</sup> Tim D. Spector,<sup>2,8,\*</sup> and Frank O. Nestle<sup>3,4,8</sup>

<sup>1</sup>ImmunoTechnology Section, Vaccine Research Center, NIAID, NIH, Bethesda, MD 20892, USA

<sup>2</sup>Department of Twin Research & Genetic Epidemiology, King's College London, London SE1 7EH, UK

<sup>3</sup>Cutaneous Medicine Unit, St. John's Institute of Dermatology, King's College London, London SE1 9RT, UK

<sup>4</sup>NIHR Biomedical Research Centre at Guy's and St. Thomas' NHS Foundation Trust, London SE1 9RT, UK

<sup>5</sup>Present address: Translational and Correlative Sciences Laboratory, Translational Research Program, Perelman School of Medicine, The University of Pennsylvania, Philadelphia, PA 19104, USA

<sup>6</sup>Present address: Division of Molecular Immunology, MRC National Institute for Medical Research, Mill Hill, London NW1 7AA, UK

<sup>7</sup>Co-first author

<sup>8</sup>Co-senior author

\*Correspondence: [roederer@nih.gov](mailto:roederer@nih.gov) (M.R.), [tim.spector@kcl.ac.uk](mailto:tim.spector@kcl.ac.uk) (T.D.S.)

<http://dx.doi.org/10.1016/j.cell.2015.02.046>

## SUMMARY

Despite recent discoveries of genetic variants associated with autoimmunity and infection, genetic control of the human immune system during homeostasis is poorly understood. We undertook a comprehensive immunophenotyping approach, analyzing 78,000 immune traits in 669 female twins. From the top 151 heritable traits (up to 96% heritable), we used replicated GWAS to obtain 297 SNP associations at 11 genetic loci, explaining up to 36% of the variation of 19 traits. We found multiple associations with canonical traits of all major immune cell subsets and uncovered insights into genetic control for regulatory T cells. This data set also revealed traits associated with loci known to confer autoimmune susceptibility, providing mechanistic hypotheses linking immune traits with the etiology of disease. Our data establish a bioresource that links genetic control elements associated with normal immune traits to common autoimmune and infectious diseases, providing a shortcut to identifying potential mechanisms of immune-related diseases.

## INTRODUCTION

The immune system has evolved over millions of years into a remarkable defense mechanism with rapid and specific protection of the host from major environmental threats and pathogens. Such pathogen encounters have contributed to a selection of immune genes at the population level that determine not only host-specific pathogen responses but also susceptibility to autoimmune disease and immunopathogenesis. Understanding how such genes interplay with the environment to determine im-

mune protection and pathology is critical for unravelling the mechanisms of common autoimmune and infectious diseases and future development of vaccines and immunomodulatory therapies.

Studies of rare disease established major genes, and their associated pathways, that regulate pathogen-specific immune responses (Casanova and Abel, 2004) and genome-wide association studies (GWAS) of autoimmune disease have also been productive for finding common variants (Cotsapas and Hafler, 2013; Parkes et al., 2013; Raj et al., 2014). Despite this progress, there are still major limitations in our understanding of the genetics of complex autoimmune or infectious diseases. A key missing piece is the elucidation of the genes controlling critical components of a normal human immune system under homeostatic conditions. These include the relative frequencies of circulating immune cell subsets and the regulation of cell-surface expression of key proteins that we expect have strong regulatory mechanisms.

Previous studies in humans and rodents have shown that variation in the levels of circulating blood T cells is in part heritable (Amadori et al., 1995; Kraal et al., 1983). Identifying the underlying genetic elements would help us understand the mechanisms of homeostasis—and its dysregulation. Twin studies are ideal to quantify the heritability of immune traits in healthy humans by allowing adjustment for the influence of genes, early environment, age, and cohort, plus a number of known and unknown confounders (van Dongen et al., 2012). Early studies from our group demonstrated genetic control of CD8 and CD4 T cell levels in twins (Ahmadi et al., 2001), and others have shown similar heritable effects in non-twins and rodents and with broad white cell phenotypes (Amadori et al., 1995; Clementi et al., 1999; Damoiseaux et al., 1999; Evans et al., 1999; Ferreira et al., 2010; Hall et al., 2000; Kraal et al., 1983; Nalls et al., 2011; Okada et al., 2011). A recent study, with a family design, was the first to perform GWAS on a larger range of immune subtypes. The authors analyzed 272 correlated immune traits derived from 95

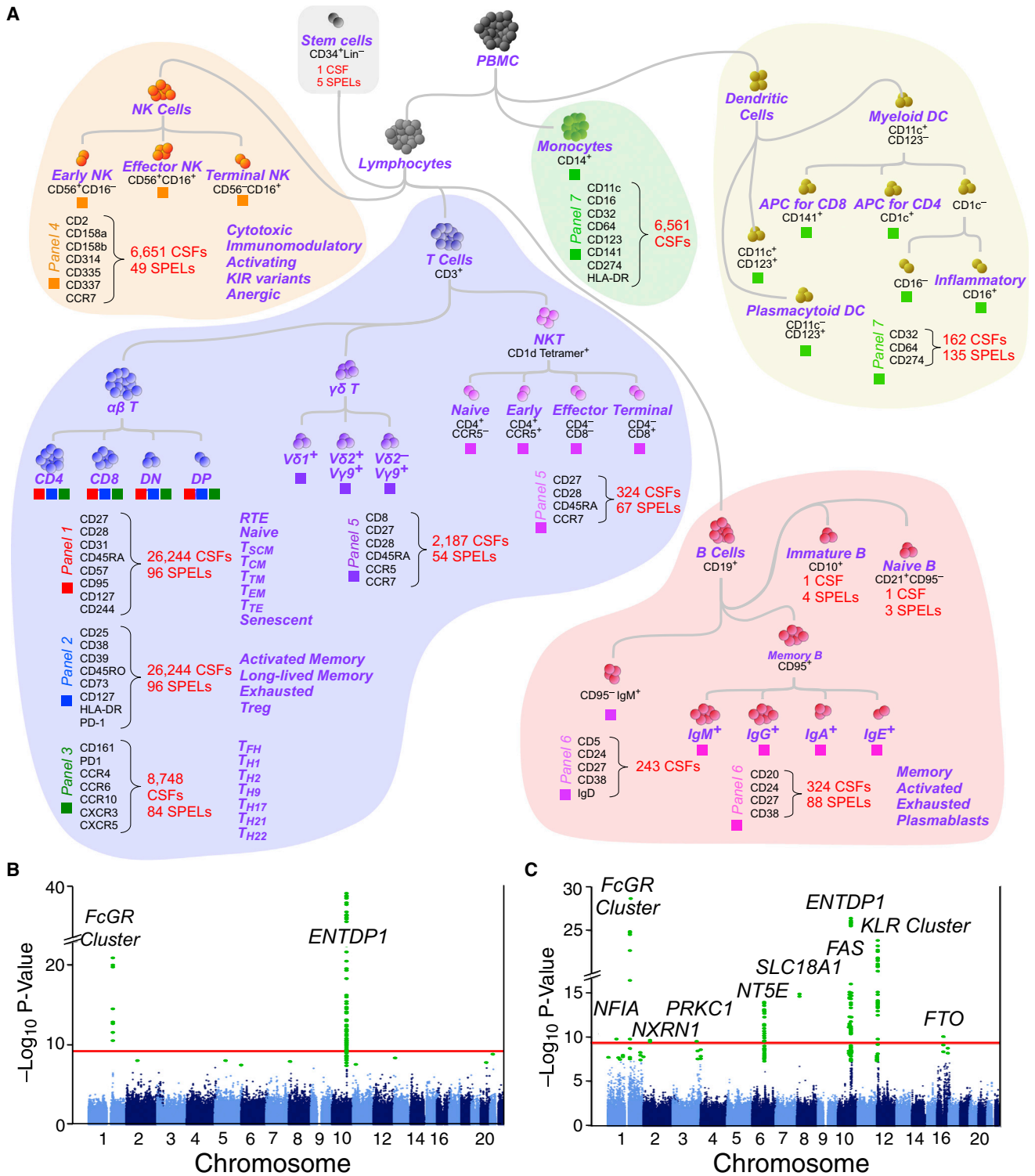


**Figure 1. Schematic Representation of Leukocyte Populations Analyzed and Summary Manhattan Plot**

(A) This diagram illustrates the approach to analyzing the immunophenotyping data obtained by flow cytometry. It is not meant to convey differentiation stages of leukocyte populations, though that property is largely reflected in this diagram. Each “lineage” of a subset of leukocytes was identified through hierarchical gating. Within each of these lineages, all possible combinations of markers with heterogeneous expression within the lineage were analyzed. The number of subsets identified by this combinatorial approach is shown in various lineages; the trait analyzed was the CSF within its parent lineage. In addition, the cell SPEL was quantified by the median fluorescence intensity of the antibody staining on a given cell subset; the number of SPEL traits is indicated as well.

(legend continued on next page)

cell types and described 23 independent genetic variants within 13 independent loci (Orrù et al., 2013).

Here, we report a comprehensive and high-resolution deep immunophenotyping flow cytometry analysis in 669 female twins using 7 distinct 14-color immunophenotyping panels that captured nearly 80,000 cell types (comprising ~1,800 independent phenotypes) to analyze both immune cell subset frequency (CSF) and immune cell-surface protein expression levels (SPELs). This gave us a roughly 30-fold richer view of the healthy immune system than was previously achievable. Taking advantage of the twin model, we used a pre-specified analysis plan that prioritized 151 independent immune traits for genome-wide association analysis and replication.

We find 241 genome-wide significant SNPs within 11 genetic loci, 9 of which are previously unreported. Importantly, they explain up to 36% of the variation of 19 immune traits (18 previously unexplored). We identify pleiotropic “master” genetic loci controlling multiple immune traits and key immune traits under tight genetic control by multiple genetic loci. In addition, we show the importance of quantifying cell-surface antigen expression rather than just cell-type frequency.

Critically, we show overlap between these genetic associations of normal immune homeostasis with previously established autoimmune and infectious disease associations. This rich database provides a vital, publicly accessible bioresource as a bridge between genetic and immune discoveries that will expedite the identification of disease mechanisms in autoimmunity and infection.

## RESULTS

### Subjects

The discovery stage comprised 497 female participants from the UK Adult Twin Register (TwinsUK). There were 75 complete monozygotic (MZ) twin pairs, 170 dizygotic (DZ) pairs, and 7 singletons (arising from quality control [QC] failures in one co-twin). The mean age was 61.4 years (range: 40–77). The replication stage comprised a further 172 participants, mean age 58.2 years (range: 32–83), with 46 MZ, 118 DZ, and 8 singletons. We stained cryopreserved peripheral blood mononuclear cells (PBMC) from each, using a set of 7 14-color immunophenotyping panels that delineate a large range of immune subsets (Figures 1A, S1, S2, and S3 and Table S1). Immune traits analyzed included the CSF (i.e., the proportionate representation of a given phenotype) and the SPEL (i.e., a quantitative measure of gene expression on a per-cell basis). The variability of all traits was assessed using longitudinal sampling on a small cohort of individuals as described in the Experimental Procedures; of the 50,000 traits meeting the first filter criterion (Figure S4), the mean covariance across samples drawn 6 months apart is 0.86. All trait values and summary analyses, including variability, are available for download. Data and statistical analysis of the discovery stage was completed per a pre-defined statistical

analysis plan before samples from the replication stage were thawed.

GWAS analysis of all 78,000 immune traits is computationally prohibitive and would require a multiple comparisons correction that dramatically reduces sensitivity. The ability to infer heritability (proportion of variance explained solely by genetic factors) by the use of twins dramatically enhanced our ability to focus on those that are most likely to be informative. Co-variation of all traits was computed; about 1,800 were independent at  $r < 0.7$  (Figure S4).

We found no significant association of the analyzed traits with self-reported tobacco use or alcohol consumption and so did not include those behaviors as covariates. We identified many traits associated with age and included age as a covariate in all analyses. Notably, an advantage of using a twin-based cohort is to render age and other cohort effects minimally impactful. The age range of our cohort was optimal for our goal of identifying immune traits associated with genetic elements that show a risk for autoimmune diseases. Because incidence for such diseases often increases with age, the greatest power for such correlations will be obtained using samples measurements most proximal to the common onset of disease.

### Heritability

Falconer’s traditional formula (twice the difference in intraclass correlations) was used to roughly estimate the heritabilities of all 78,000 immune traits; after ranking, traits were selected for further pre-specified analyses (Figure S4). Variance components analysis (additive genetics, common environment, and unique environment, or ACE model) was used to more precisely estimate heritabilities of chosen traits. The heritabilities ranged widely from 0%—suggesting purely environmental or stochastic influences—to 96% (e.g., CD32 expression on dendritic cells), indicating a strong genetic effect. Figure S5 shows the range of heritabilities for selected traits, and the components of the model are tabulated in Table S2 with full trait descriptions.

### GWAS of Immune Traits

Single-variant associations were performed on 151 immune traits selected for high heritability or biological interest, comprising cell frequency (129 CSFs) and cell-surface protein expression (22 SPELs). Many significant associations were found despite the stringent Bonferroni multiple testing threshold of  $p < 3.3 \times 10^{-10}$ . We also performed a conditional analysis, including the top SNP of each locus as a covariate, to identify potential independent secondary signals. This analysis did not reveal any significant evidence for additional independent signals.

Six SPELs were significant (Table 1), with the strongest between MFI:516 (CD39 SPEL on CD4 T cells) and the *ENTPD1* (CD39 gene) SNP rs7096317 ( $p = 9.4 \times 10^{-40}$ ). Many other variants of *ENTPD1* were also associated with this trait (Table S3). Expression of five others (MFI:189, MFI:212, MFI:231, MFI:504, and MFI:552, which include CD27 expression on B and T cell

(B and C) Summary Manhattan plots: green dots, genome-wide significant associations ( $p < 5 \times 10^{-8}$ ). The red line indicates the significance threshold of  $p < 3.3 \times 10^{-10}$ , which corresponds to the standard genome-wide threshold after further adjustment for 151 independent tests. The variants shown are MAF  $\geq 0.1$ ; call rate  $\geq 0.9$ ; HWE  $p$  value  $\geq 1 \times 10^{-8}$ . Shown are separate plots for SPEL associations (B) and CSF associations (C).

**Table 1. Discovery and Replication Results for the Top Significant SNPs at Each Locus for Each Immune Trait**

Locus:Genes	Trait ID	Trait Phenotype	Marker	Chr	EA/NEA	EAF	Beta (SE)	p Value	Beta (SE)	p Value	Beta (SE)	p Value
1: <i>FCGR2A, FCGR2B, FCRLA</i>	MFI:189	CD27 on IgA <sup>+</sup> B	rs1801274	1	A/G	0.49	0.128 (0.02)	6.48E−11	0.07 (0.03)	3.70E−02	0.11 (0.02)	2.8E−11
1: <i>FCGR2A, FCGR2B, FCRLA</i>	MFI:212	CD27 on IgG <sup>+</sup> B	rs1801274	1	A/G	0.49	0.136 (0.02)	5.38E−12	0.12 (0.03)	1.11E−04	0.13 (0.02)	2.9E−15
1: <i>FCGR2A, FCGR2B, FCRLA</i>	MFI:231	CD161 on CD4 T	rs1801274	1	A/G	0.49	0.131 (0.02)	2.64E−11	0.12 (0.03)	2.17E−04	0.13 (0.02)	2.7E−14
1: <i>FCGR2A, FCGR2B, FCRLA</i>	MFI:504	CD27 on CD4 T	rs1801274	1	A/G	0.49	0.145 (0.02)	5.42E−14	0.14 (0.03)	4.20E−05	0.14 (0.02)	1.1E−17
1: <i>FCGR2A, FCGR2B, FCRLA</i>	MFI:552	CD27 on CD8 T	rs1801274	1	A/G	0.49	0.186 (0.02)	1.26E−21	0.12 (0.03)	1.72E−04	0.17 (0.02)	4.2E−24
1: <i>FCGR2A, FCGR2B, FCRLA</i>	P7:110	iMDC: %CD32 <sup>+</sup>	rs10494359	1	C/G	0.12	0.343 (0.03)	2.52E−29	0.43 (0.05)	1.05E−15	0.36 (0.03)	5.9E−43
1: <i>FCGR2A, FCGR2B, FCRLA</i>	P7:224	CD1c <sup>+</sup> mDC: %CD32	rs4657090	1	A/G	0.27	−0.174 (0.02)	1.30E−14	−0.19 (0.04)	3.86E−06	−0.18 (0.02)	2.7E−19
2: <i>NFIA</i>	P4:3551	NK: %CD314 <sup>−</sup> CD158a <sup>+</sup>	rs12072379	1	G/C	0.16	−0.131 (0.02)	1.73E−10	−0.10 (0.05)	4.87E−02	−0.13 (0.02)	2.7E−11
3: <i>NRXN1</i>	P4:3551	NK: %CD314 <sup>−</sup> CD158a <sup>+</sup>	rs17040907	2	T/C	0.07	−0.208 (0.03)	2.68E−10	−0.16 (0.08)	4.22E−02	−0.02 (0.03)	3.9E−11
4: <i>PRKCI</i>	P4:3551	NK: %CD314 <sup>−</sup> CD158a <sup>+</sup>	rs2650220	3	G/A	0.16	−0.15 (0.02)	3.18E−10	−0.10 (0.05)	4.55E−02	−0.14 (0.02)	6.0E−11
5: <i>NT5E</i>	P2:4195	CD4 T: %CD39 <sup>−</sup> CD73 <sup>+</sup>	rs9444346	6	G/A	0.19	−0.2 (0.03)	1.18E−14	−0.12 (0.04)	4.98E−03	−0.18 (0.02)	8.8E−16
<i>RP11-30P6</i>	P2:4204	CD4 T: %CD73 <sup>+</sup>	rs9444346	6	G/A	0.19	−0.195 (0.03)	5.85E−14	−0.12 (0.04)	2.82E−03	−0.18 (0.02)	1.8E−15
6: <i>SLC18A1</i>	P4:3551	NK: %CD314 <sup>−</sup> CD158a <sup>+</sup>	rs1390942	8	T/C	0.15	−0.163 (0.02)	1.39E−15	−0.20 (0.05)	1.70E−04	−0.17 (0.02)	1.4E−18
7: <i>SLC25A16</i>	P4:3551	NK: %CD314 <sup>−</sup> CD158a <sup>+</sup>	rs3017072	10	T/C	0.15	−0.153 (0.02)	2.75E−13	−0.15 (0.05)	2.08E−03	−0.15 (0.02)	2.2E−15
8: <i>FAS, ACTA2</i>	P1:6601	CD8 T: %TSCM	rs7097572	10	C/T	0.48	−0.168 (0.02)	8.51E−16	−0.18 (0.03)	2.72E−06	−0.17 (0.02)	1.3E−20
9: <i>ALDH18A1, ENTPD1, ENTPD1-AS1, RP11-7D5, SORBS1, TCTN3</i>	MFI:516	CD39 on CD4 T	rs7096317	10	G/A	0.42	−0.255 (0.02)	9.40E−40	−0.30 (0.04)	9.92E−17	−0.27 (0.02)	1.6E−54
9: <i>ALDH18A1, ENTPD1, ENTPD1-AS1, RP11-7D5, SORBS1, TCTN3</i>	P2:10491	CD8 T: %CD39 <sup>+</sup>	rs4074424	10	G/C	0.42	−0.219 (0.02)	4.11E−27	−0.19 (0.04)	2.40E−07	−0.21 (0.02)	8.2E−33
9: <i>ALDH18A1, ENTPD1, ENTPD1-AS1, RP11-7D5, SORBS1, TCTN3</i>	P2:3460	CD4 T: %CD39 <sup>+</sup> CD38 <sup>+</sup> PD1 <sup>−</sup>	rs4582902	10	C/T	0.47	−0.164 (0.02)	4.55E−16	−0.19 (0.03)	2.58E−08	−0.17 (0.02)	9.2E−23
9: <i>ALDH18A1, ENTPD1, ENTPD1-AS1, RP11-7D5, SORBS1, TCTN3</i>	P2:4159	CD4 T: %CD39 <sup>+</sup> CD73 <sup>−</sup>	rs6584027	10	G/A	0.47	−0.212 (0.02)	1.54E−25	−0.20 (0.04)	1.09E−08	−0.21 (0.02)	1.1E−32
9: <i>ALDH18A1, ENTPD1, ENTPD1-AS1, RP11-7D5, SORBS1, TCTN3</i>	P2:4186	CD4 T: %CD39 <sup>+</sup>	rs6584027	10	G/A	0.47	−0.215 (0.02)	2.20E−26	−0.21 (0.04)	5.27E−09	−0.21 (0.02)	7.8E−34
9: <i>ALDH18A1, ENTPD1, ENTPD1-AS1, RP11-7D5, SORBS1, TCTN3</i>	P2:4213	CD4 T: %CD39 <sup>+</sup> CD73 <sup>+</sup>	rs10882676	10	A/C	0.47	−0.195 (0.02)	6.76E−22	−0.19 (0.04)	2.19E−07	−0.19 (0.02)	9.0E−28
10: <i>KLRC1, KLRC2, KLRC4, KLRK1, RP11-277P12</i>	P4:3551	NK: %CD314 <sup>−</sup> CD158a <sup>+</sup>	rs2734565	12	C/T	0.3	−0.144 (0.02)	1.34E−10	−0.18 (0.04)	1.67E−05	−0.15 (0.02)	1.4E−14
10: <i>KLRC1, KLRC2, KLRC4, KLRK1, RP11-277P12</i>	P4:4832	NK: %CD314 <sup>−</sup> CCR7 <sup>−</sup>	rs2734565	12	C/T	0.3	−0.233 (0.02)	1.27E−24	−0.33 (0.04)	3.95E−15	−0.26 (0.02)	2.7E−37
10: <i>KLRC1, KLRC2, KLRC4, KLRK1, RP11-277P12</i>	P4:5538	NK: %CD314 <sup>−</sup> CD335 <sup>+</sup>	rs2734565	12	C/T	0.3	−0.275 (0.02)	3.40E−34	−0.38 (0.04)	2.27E−19	−0.30 (0.02)	6.4E−51
11: <i>FTO</i>	P4:3551	NK: %CD314 <sup>−</sup> CD158a <sup>+</sup>	rs1420318	16	A/G	0.1	−0.146 (0.02)	9.34E−11	−0.19 (0.06)	4.05E−02	−0.14 (0.02)	1.2E−11

For the Discovery stage, we used a significance threshold of  $p < 3.3 \times 10^{-10}$ . This threshold corresponds to the standard genome-wide threshold of  $5 \times 10^{-8}$  after further adjustment for 151 independent tests. Orrù et al. (2013) also identified Locus 1 (associated with a single trait, CD62L<sup>−</sup> dendritic cells, not measured in our panel), and Locus 9 (associated with a single trait: CD39<sup>+</sup> CD4 T cell frequency, P2:4186 in our list). The trait ID is fully described in Table S2.

subsets, and CD161 expression on CD4 T cells) were associated with variants on chromosome 1q23 in a genetic region containing the important immune-regulating genes *FCGR2A*, *FCGR2B*, and *FCRLA* (Table 1). These associations were independently verified in the replication cohort, and the combined discovery and replication set p values of the 6 SPELs ranged from  $2.8 \times 10^{-11}$  to  $1.6 \times 10^{-54}$  (Table 1 and Figure 1B). Table S3 illustrates other examples of genetic control of cell-surface expression, including the expression of CD11c, CD123, and CD274 on myeloid subsets.

Overall, 241 SNP variants with a minor allele frequency above 5% were significantly associated with various SPELs (Table S3); of these, 35 SNPs were pleiotropically associated with multiple SPELs.

Genetic control of SPEL may simply be due to promoter/enhancer element variants or more complex regulation of transcription, translation, or protein localization. In contrast, genetic control of CSF may reveal homeostatic mechanisms regulating cell subset representation in the blood. Genome-wide significant associations were identified with 13 different CSFs (Figure 1C and Table 1). Nearly all were verified in the replication cohort (Table 1), and some reached a p value of  $10^{-43}$ .

Suggestive associations, which did not meet the conservative significance threshold of  $3.3 \times 10^{-10}$ , were also identified for numerous SPELs and CSFs (Tables S3 and S4). The associations that were independently replicated (replication  $p < 0.05$ ), as well as meta-analyzed variants reaching  $p < 5 \times 10^{-8}$ , are reported in Table S6.

### Genetic Control of T<sub>REG</sub> Cells

One of the most heritable traits identified from our staining panels was the frequency of CD39<sup>+</sup> cells within the CD4 compartment (Figure 2), as previously reported (Orrù et al., 2013). CD39<sup>+</sup>CD4 T, as well as CD73<sup>+</sup> CD4 T cells, have been identified functionally as T regulatory (T<sub>REG</sub>) cells (Borsellino et al., 2007), a key subset in the modulation of immune responses (Antonioli et al., 2013).

The heritability of CD39<sup>+</sup>CD4 T frequency was 89% (95% CI: 66%–93%) (Figure 2A). GWAS analysis revealed a single locus on chromosome 10 that was highly associated with the trait (Figure 2B); this locus maps to the CD39 gene itself. Quantification of the expression of CD39 on a per-cell basis (i.e., SPEL) revealed that the basis for this association was an “on/off” control of the expression of the CD39 molecule on the cells, rather than a homeostatic regulation of the circulating levels of these cells (i.e., CSF). Specifically, individuals who are homozygous for rs7096317A express the highest amount of this protein on the cell surface; heterozygotes expressed half as much; and rs7096317G homozygotes expressed virtually none (Figures 2C and 2D). Although the A/G heterozygotes have a significantly decreased CD39 SPEL, the cells express enough so as to remain CD39<sup>+</sup>. Thus, in the analysis of the CD39 CSF by genotype, only the G/G homozygotes have a reduced frequency of this population (Figure 2E). This illustrates the power of the SPEL analysis to de-convolute potential mechanisms of genetic control that are missed by simple analysis of CSF.

Similarly, the frequency of CD4 T cells that are CD25<sup>+</sup>CD127<sup>-</sup>CD45RO<sup>+</sup> but do not express CD39 was also strongly associ-

ated with this same locus, showing the opposite association (Figure 2F). In other words, genetic control is not over the frequency of T<sub>REG</sub> (CD4<sup>+</sup>CD25<sup>+</sup>CD127<sup>-</sup>CD45RO<sup>+</sup>) but over the quantitative expression of CD39 (the cell phenotype). Notably, this genetic control also extends to lymphocytes that are not T<sub>REG</sub>: a similar genotypic association (Figure S6) was found for the relatively rare CD8<sup>+</sup> and CD4<sup>-</sup>CD8<sup>+</sup> T cells expressing CD39 (Figures S7A and S7B). Finally, CD73 is an ectonuclease similar to CD39, and its expression has also been associated with T<sub>REG</sub> cells (Antonioli et al., 2013). The expression of CD73 was also found to be genetically controlled (Figure S7C) and associated with a single locus on chromosome 6 mapping to the CD73 gene itself.

Thus, the main genetic control of CD39<sup>+</sup> T<sub>REG</sub> appears to originate from a transcriptional or post-transcriptional regulation leading to the presence or absence of this protein on the cell surface of T<sub>REG</sub> cells; for those T<sub>REG</sub> defined on a basis independent of CD39, we found no evidence of genetic control over their representation in blood.

### Genetic Influences on Leukocyte Differentiation

In virtually every leukocyte population, we found examples in which the frequency of certain differentiation stages was heritable (Figure 3). In some cases, despite a very high heritability, we were unable to identify genetic variants that correlated with the trait. For example, the frequency of a CD4 transitional memory (T<sub>TM</sub>) phenotype (CD28<sup>+</sup>CD127<sup>-</sup>), which comprises 15% to 20% of CD4 T cells, was very strongly heritable (Figure 3A) but did not correlate with any SNP genotypes. We found similar examples of strong heritability without genetic associations for other T cell stages, including recent thymic emigrants (RTE) and central memory (T<sub>CM</sub>). This was not unexpected—our study was only powered to find large effect sizes of gene variants, which is unusual for most traditional disease GWASs that need thousands of subjects per association. This suggests that possibly multiple genes of modest influence act on these phenotypes. Despite the lack of defined genetic association, the observation of strong heritability indicates that these cell types play an important and unique role in immunity, such that their numbers are strongly regulated.

For a number of leukocyte lineages, we were able to identify genetic associations with differentiation stages and illustrate four examples. (1) Within B cells, the proportion that is immature (CD10<sup>+</sup>) is associated with the genotype of the membrane metallo-endopeptidase (*MME*) gene (Figure 3B). (2) The proportion of Th22 CD4 T cells (CXCR3<sup>+</sup>CCR4<sup>+</sup>CCR6<sup>+</sup>CCR10<sup>+</sup>) is strongly associated with a single locus on chromosome 16, mapping to the *SPG7* gene, which codes for paraplegin, an important protein in mitochondrial function (Figure 3C). (3) Within natural killer (NK) cells, the proportion of cells that express CD335 but not CD314 (Figure 3D) maps to the *KLRC4* gene (Figure 3E). This association is much more profound for NK cells that are in an early differentiation stage (CD56<sup>+</sup>CD16<sup>-</sup>) and becomes less strong as the cells mature (Figure 3F). This indicates that a mechanism evinced in a differentiation stage-specific manner. (4) The proportion of T cells that are “stem cell memory” cells (T<sub>SCM</sub>; the earliest memory stage) is heritable (Figure 3G) and associated with a genetic locus containing *FAS* (CD95) (Figure 3H). This

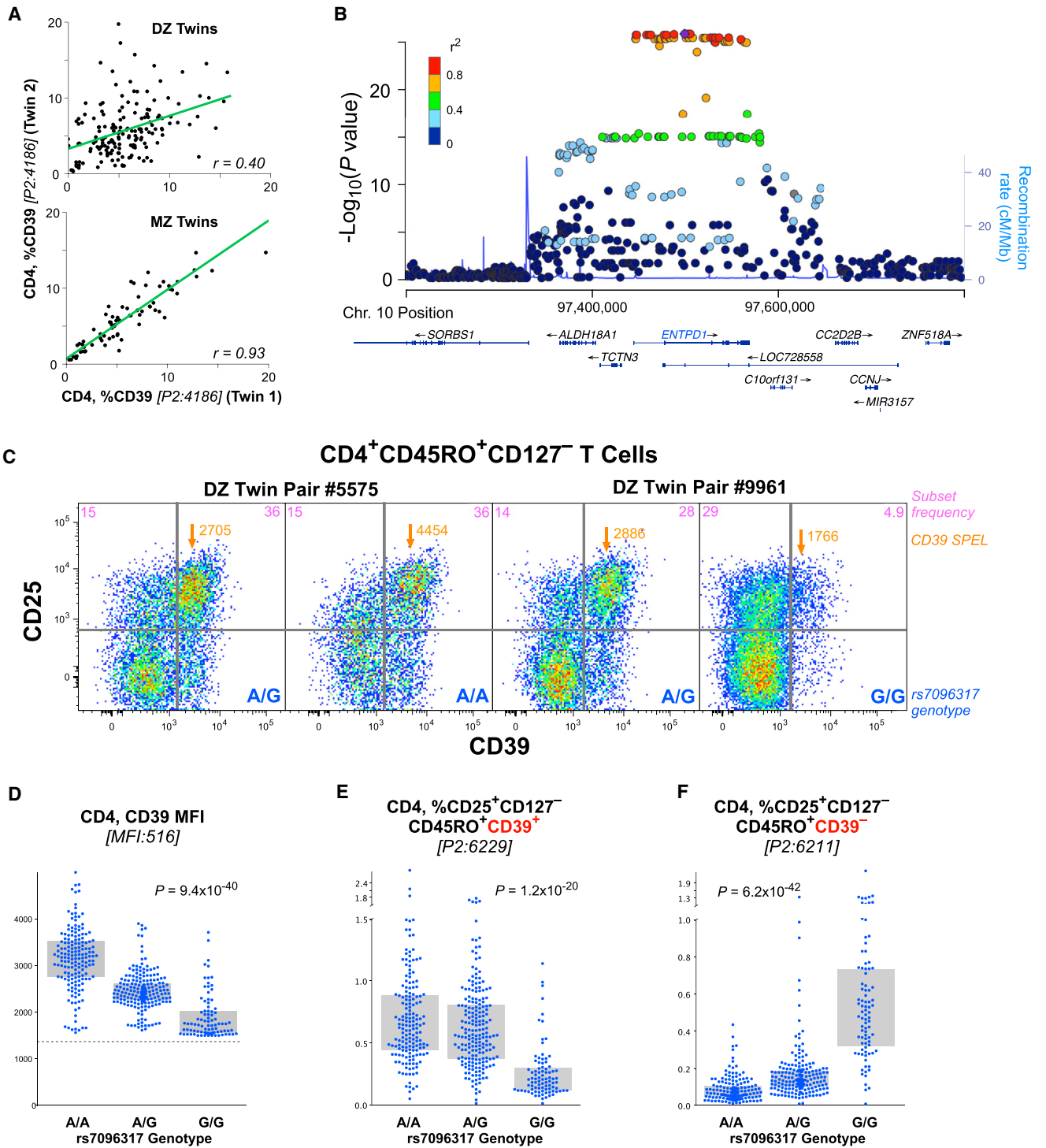


**Figure 2. Genetic Associations with Treg Phenotype Cells**

(A) The correlation of the fraction of CD4 T cells that are CD39<sup>+</sup> in dizygotic twins (top) and monozygotic twins (bottom). The linear correlation, *r*, is shown for each comparison.

(B) Locus plot showing significant effect of individual SNPs on CD39 expression on CD4 T cells.

(C) Shown are the expression profiles of CD39 and CD25 for the subset of CD4 T cells that are CD45RO<sup>+</sup>CD127<sup>-</sup> for two pairs of dizygotic twins discordant for the rs7096317 allele (in the CD39 gene locus). Within each graphic is shown the fraction of cells in the upper two quadrants and the surface protein expression level (SPEL) of CD39 for the cells in the upper right quadrant, as well as the genotype of each individual.

(legend continued on next page)

association was much stronger for CD4 than for CD8 T cells.  $T_{SCM}$  are precursor cells that have tremendous proliferative capacity and can regenerate all other memory T cell populations (Gattinoni et al., 2011; Lugli et al., 2013). Interestingly, this same locus also has a significant association with the fraction of T cells that are CD8 (Figure 3I), demonstrating multiple (pleiotropic) effects of the FAS gene on T cell differentiation.

### Pleiotropic Impact of the FcRG2 Locus

The locus with the widest range of impacts on leukocyte subset phenotype and frequency was on chromosome 1, a region including the FcRG2 gene. This locus is well known for its association with a variety of autoimmune and inflammatory diseases, including systemic lupus erythematosus (SLE), Kawasaki's disease, inflammatory bowel disease, Crohn's disease, type 1 diabetes, and HIV disease progression. Despite the genes in this locus being primarily expressed on myeloid and B lymphoid cells, many of these diseases are traditionally associated with T cell dysregulation.

The strongest association (e.g., SNP rs1801274) we identified for this locus was with the expression of CD32 (FcRG2a and/or FcRG2b: these are indistinguishable by the monoclonal antibody used in our panel) on the surface of inflammatory myeloid dendritic cells (imDC; Figures 4A and 4B). The heritability of this trait was extremely high at 96% (CI: 81%–97%).

The genetic control of the expression of CD32 on imDCs was not seen in all cell populations. For example, B cells showed no control (Figure 4C), whereas the expression of CD32 on imDCs is associated with the number of rs1801274 "T" alleles (Figures 4C and 4D).

The rs1801274 genotype has been strongly associated with susceptibility to SLE, as well as another SNP in the same locus, rs10800309. This latter SNP has also been associated with ulcerative colitis. The frequency of CD32<sup>+</sup> imDCs is strongly affected by the genotypes at both of these loci (Figures 4D and 4E); however, the distribution of expression for either locus is not uniform: high, intermediate, and low expressors can be found within all genotypes with differing frequencies. However, when the two genotypes are taken together as a diplotype, a powerful and replicated association becomes evident for CD32<sup>+</sup> imDCs (Figures 4E and S8C). The impact of this diplotype on CD32 expression extends to other myeloid subsets (Figures 4F and S8A). Statistical significance of the association is greatest for monocytes, although the dynamic range in the expression levels is not as wide as it is for imDCs. Other subsets, such as the professional antigen presenting mDC, show a muted control of expression; CD11c<sup>+</sup>CD123<sup>+</sup> DC, like B cells, show no differential regulation of CD32 expression at all.

Given the profound impact of these genotypes on particular subsets, it raises the possibility that part of the increased susceptibility to associated autoimmune diseases may be a consequence of the altered function of cells like imDCs by virtue of a differential expression of the activating (CD32a) or repressing

(CD32b) proteins that we identify here. This is perhaps driven by a SNP in the promoter/enhancer areas in high linkage disequilibrium to the commonly studied coding SNP rs1801274.

We also found a remarkable range of effects of the FcRG2 locus on a variety of lymphocyte subsets (Figure 5). For example, the proportion of early NK cells that are CD2<sup>+</sup>CD158a<sup>+</sup>CD158b<sup>+</sup> is strongly associated with SNP rs365264 (Figure 5A), located between CD32a and CD16 (Figure 4B). The rs1801274 coding SNP in the locus was associated with phenotypes on both B cells and T cells, including the fraction of memory IgG<sup>+</sup> (Figure 5B) or IgA<sup>+</sup> (Figure S8B) B cells that express CD27, as well as the CD27 expression level on a per cell basis. Interestingly, in this case, the higher surface expression levels of CD27 (SPEL) are associated with lower frequencies of cells that express CD27 (CSF). Thus, in contrast to the example of CD39<sup>+</sup> T<sub>REG</sub> (Figure 2), differential regulation of CD27 protein expression does not account for differential frequency of these cell subsets.

### T Cells, FcRG2, and Autoimmune Disease

Similar to the case for IgG<sup>+</sup> B cells, CD8 T cells also exhibited higher CD27 expression in association with rs1801274T allele (Figure 5C); this was also true for other T cell lineages (Figure S8). Furthermore, a population of CD4 T cells that express CD161 is also strongly associated with this same genotype (Figure 5D). Importantly, CD161<sup>+</sup> T cells are either Th17 or mucosal-associated innate T (MAIT) cells, important for maintenance of mucosal integrity. Thus, we define an impact of specific gene variants on important T cell phenotypes closely related to their activation potential, which may underlie the associations with T-cell-based autoimmune diseases.

Finally, Starbeck-Miller et al. (2014) recently demonstrated that CD8 T cells can express CD32b and that this expression was functionally important in modulating cytolytic T cell responses. Here, we demonstrate that expression of CD32 on CD8 T cells is low and variable between individuals (Figure 5E). Notably, this expression shows a very strong association with the rs1801274:rs10800309 diplotype of the FcRG2 gene locus (Figure 5F). This suggests that the regulation of surface expression of this negative regulatory molecule on CD8 T cells (Starbeck-Miller et al., 2014) has a common expression mechanism to that in myeloid populations. Gene variants increasing susceptibility to SLE also associate with lower levels of this negative regulatory protein on CD8 T cells and imDC. Together, these data provide a possible direct link between the SNPs highly associated with autoimmune diseases and T cell phenotypes that might account for the pathogenesis.

### Overlap with Disease Associations

The Catalog of Published Genome-wide Association Studies (<http://www.genome.gov/gwastudies/>) and ImmunoBase (<http://www.immunobase.org/>) were used to evaluate the overlap between genetic variants associated with CSFs and SPELs in our study and those reported to be suggestively or statistically

(D) The CD39 SPEL of CD39 positive cells is graphed by the genotype of rs7096317; the dotted line indicates the threshold of positivity above which a cell was considered CD39<sup>+</sup>. In the C/C genotype, relatively few cells are above this threshold and the median fluorescence intensity values are not robust.

(E and F) The fraction of CD4 T cells of the designated phenotype is graphed by the rs7096317 genotype. Bars indicate interquartile range.

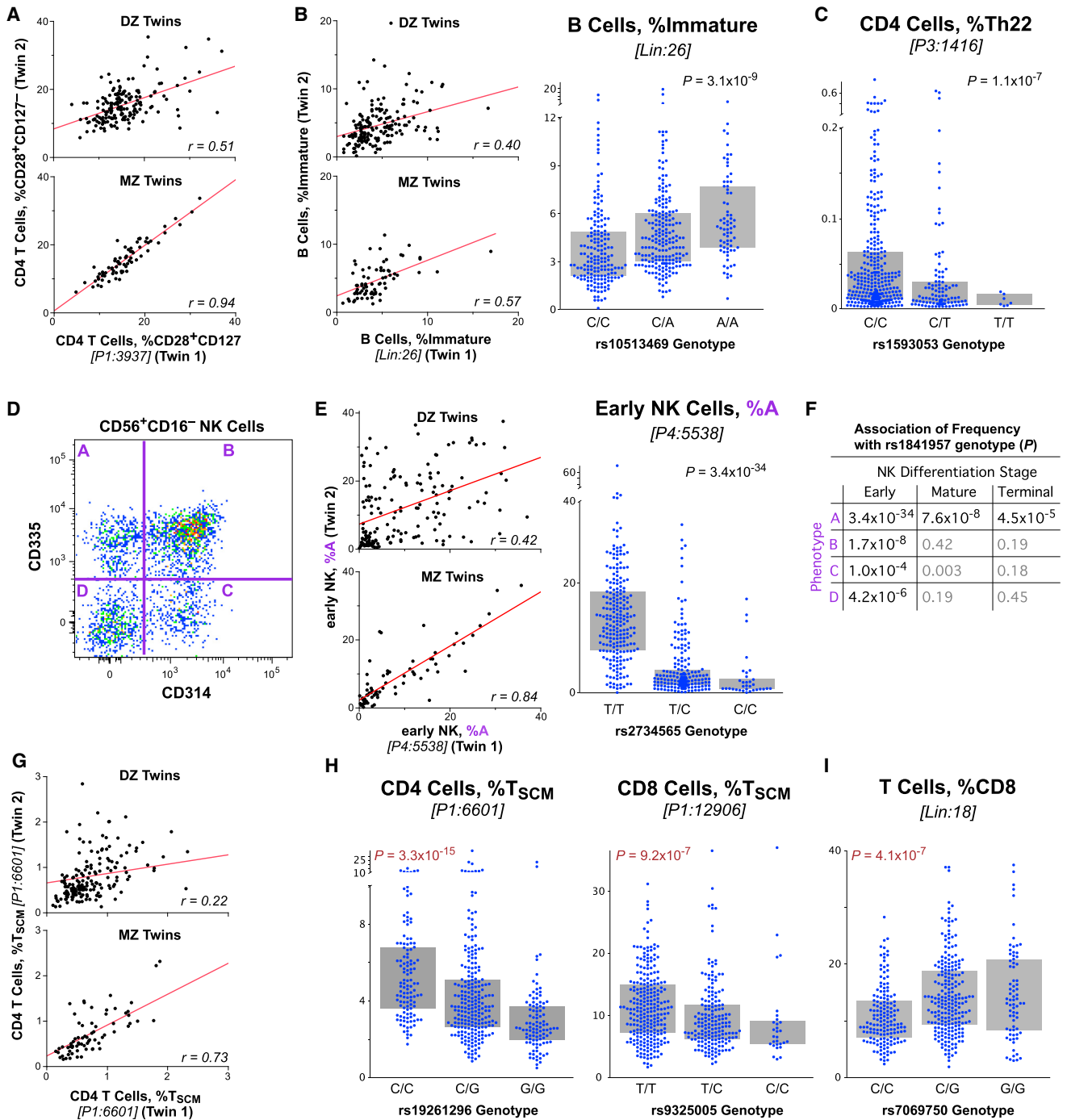


**Figure 3. Genetic Associations with Lymphocyte Differentiation**

(A) The proportion of CD4 T cells that are “translational memory” (CD28<sup>+</sup>CD127<sup>-</sup>) is shown for DZ and MZ twins.  
 (B) The proportion of B cells that are immature is shown for twins (left) and is strongly associated with the genotype of rs10513469 (MME gene) (right).  
 (C) The proportion of CD4 T cells that are Th22 (CXCR3<sup>+</sup>CCR4<sup>+</sup>CCR6<sup>+</sup>CCR10<sup>+</sup>) is associated with the genotype of rs2019604 (SPG7 gene).  
 (D) A frequency of four phenotypes within NK cells (designated as “A”...“D” based on the expression of CD314 (KLRC4) and CD335) is shown for “early” (CD56<sup>+</sup>CD16<sup>-</sup>) differentiated NK cells.  
 (E) The proportion of early NK cells that are CD314<sup>-</sup>CD335<sup>+</sup> (population “A”) is shown for DZ and MZ twins (left). (Right) The genotypes of rs1841957 (near the KLRC4/CD314 locus) strongly associate with the frequency of CD314<sup>-</sup>CD335<sup>+</sup> cells among early NK.  
 (F) The associations of rs1841957 with all four phenotypes within differentiation stages of NK cells are shown by p value.

(legend continued on next page)

significant in candidate SNP, candidate gene, or genome-wide association studies of complex and infectious diseases.

SNPs that were highly correlated variants ( $r^2 > 0.8$ ) with our significant immune traits were also interrogated for overlap with reported disease associations using the appropriate thresholds for the number of tests. A number of gene variants significantly and suggestively ( $p < 10^{-3}$ ) correlated with CSFs and SPELs have been reported in associations of complex and infectious diseases, as shown in Table 2. The different gene variants of *FCGR2A*, associated with a range of myeloid and T cell phenotypes in our data, were reported to be associated with increased risk of a number of diseases, including inflammatory bowel disease, ulcerative colitis, SLE, Kawasaki disease, ankylosing-spondylitis, and HIV progression (Table 2). An additional variant of *FCGR2A*, rs10494359 (associated with P7:100 [CD64<sup>+</sup>CD274<sup>+</sup>imDCs]), is closely correlated (in linkage disequilibrium) with rs10494360 ( $r^2 = 0.941$ ) and has been associated with rheumatoid arthritis. Juvenile idiopathic arthritis and chronic lymphocytic leukemia susceptibility loci in the *ACTA2/FAS* region of chromosome 10q23.31 were also associated with the frequency of P1:6601 (CD4 T<sub>SCM</sub>) ( $p = 4.1 \times 10^{-12}$ ; Table 2). The Behçet's disease susceptibility variant in the killer cell lectin-like receptors gene region corresponded with the frequencies of P4:3551, P4:4832, and P4:5538 (all three are CD314<sup>+</sup> subsets of NK cells). The correlations of variants association with tuberculosis, malaria, leprosy, HIV, and hepatitis B and C our immune traits are presented in Table 2.

## DISCUSSION

Understanding the fundamental principles of how the immune system protects the host from infection yet also contributes to autoimmunity and other disease pathogenesis is essential for the development of novel diagnostics and medicines. There remains a major gap in our understanding of genetic determinants of a normal human immune system and its main coordinates such as the frequency of immune cells and expression of relevant proteins. Using 669 twins and the richest immunophenotyping performed to date, we investigated the genetic architecture of immune traits. We describe multiple independent genetic variants at several genetic loci explaining a substantial proportion (up to 96%) of the genetic variation. We identify both pleiotropic genetic loci that control multiple immune traits and single immune traits under genetic influence by multiple loci. For certain canonical immune traits, genetic control is exerted at the level of immune cell-surface protein expression (i.e., a consequence of promoter/enhancer or signaling mechanisms) rather than at the level of cell subset frequency (i.e., homeostasis or differentiation mechanisms). We further describe multiple genetic associations with common canonical immune traits related to leukocyte lineage and differentiation of major immune cell subsets such as B cells, T cells, and natural killer cells. Finally, we identify genetic elements associated with both immune traits and auto-

immune and infectious diseases. Providing the heritabilities of thousands of cell subtypes plus a basis to uncover the genetic architecture of the numerous gene-immune associations establishes this data set as an essential bioresource for researchers. The remarkably strong associations we find for genetic traits linked to disease illustrate the power of our approach by using twins and optimized high-quality immune phenotyping.

Some limitations of our study should be noted: the cohort used is all female, it is (for GWAS) a relatively limited sample size, and it is relatively homogeneous in terms of environmental exposure. The low numbers of genetic associations on chromosome 6 (the major histocompatibility region) is possibly explained by the considerable complexity and polymorphism in this gene region, which would require larger sample sizes to obtain statistically significant genetic associations. With regard to immunological traits, it should be noted that our discovery cohort ranges in age from 41 to 77. It is possible that analysis of a younger cohort, for which less environmental pressure on the immune system has occurred, would reveal stronger associations; on the other hand, it is likely that the greatest power to detect immune correlates related to disease will come from measurements at a time most proximal to the typical onset. Nevertheless, our success in identifying a large number of genetic variants with genome-wide significance validates our approach of focusing on well-defined and curated immune phenotypes. It should be noted that the 297 SNPs we report (Table S5) are those that attained genome-wide significance (with a conservative correction for multiple comparisons) in both the discovery and replication cohorts. Many more associations are evident in the data set (e.g., Tables S2 and S3), which can serve to formulate new testable hypotheses and genetic studies.

An example of the power of the resource was in distinguishing two important mechanisms that lead to differential representation of immune cell phenotypes (e.g., CD39<sup>+</sup> CD4 T cells). The first is homeostatic—i.e., mechanisms that control the recirculation, proliferation, and elimination of a certain cell type in the blood—a cellular mechanism expressed at the whole-body level. Such mechanisms, although unidentified, are known to exist for regulating major subset numbers (such as CD4 T cell numbers). A second, completely independent mechanism is the molecular regulation of the protein expression at the cell level itself (e.g., promoter/enhancer variants). Thus, even in the presence of intact homeostatic mechanisms regulating that cell type, a reduction in the number of cells expressing a protein (perhaps part of the defining phenotype) may be due to a specific promoter variant that simply abrogates the expression of the gene. Here, we show examples of both mechanisms.

An example of a major immune trait under genetic control is the phenotype, but not frequency, of regulatory T (T<sub>REG</sub>) cells. T<sub>REG</sub> cells are essential for maintenance of immune homeostasis, and their dysregulation might lead to autoimmunity (Sakaguchi et al., 2010). A pleiotropic locus containing the ectonucleoside triphosphate diphosphohydrolase 1 (*ENTPD1* and CD39)

(G) The proportion of CD4 T cells that are "stem cell memory" (T<sub>SCM</sub>: CD45RA<sup>+</sup>CD95<sup>+</sup>CD27<sup>+</sup>CD28<sup>+</sup>CD127<sup>+</sup>CD57<sup>-</sup>) is shown for DZ and MZ twins.

(H and I) The genotypes of rs7069750 (FAS gene) are associated with the proportion of CD4 and CD8 T cells that are T<sub>SCM</sub>, as well as the proportion of all T cells that are CD8.

Bars indicate interquartile ranges.

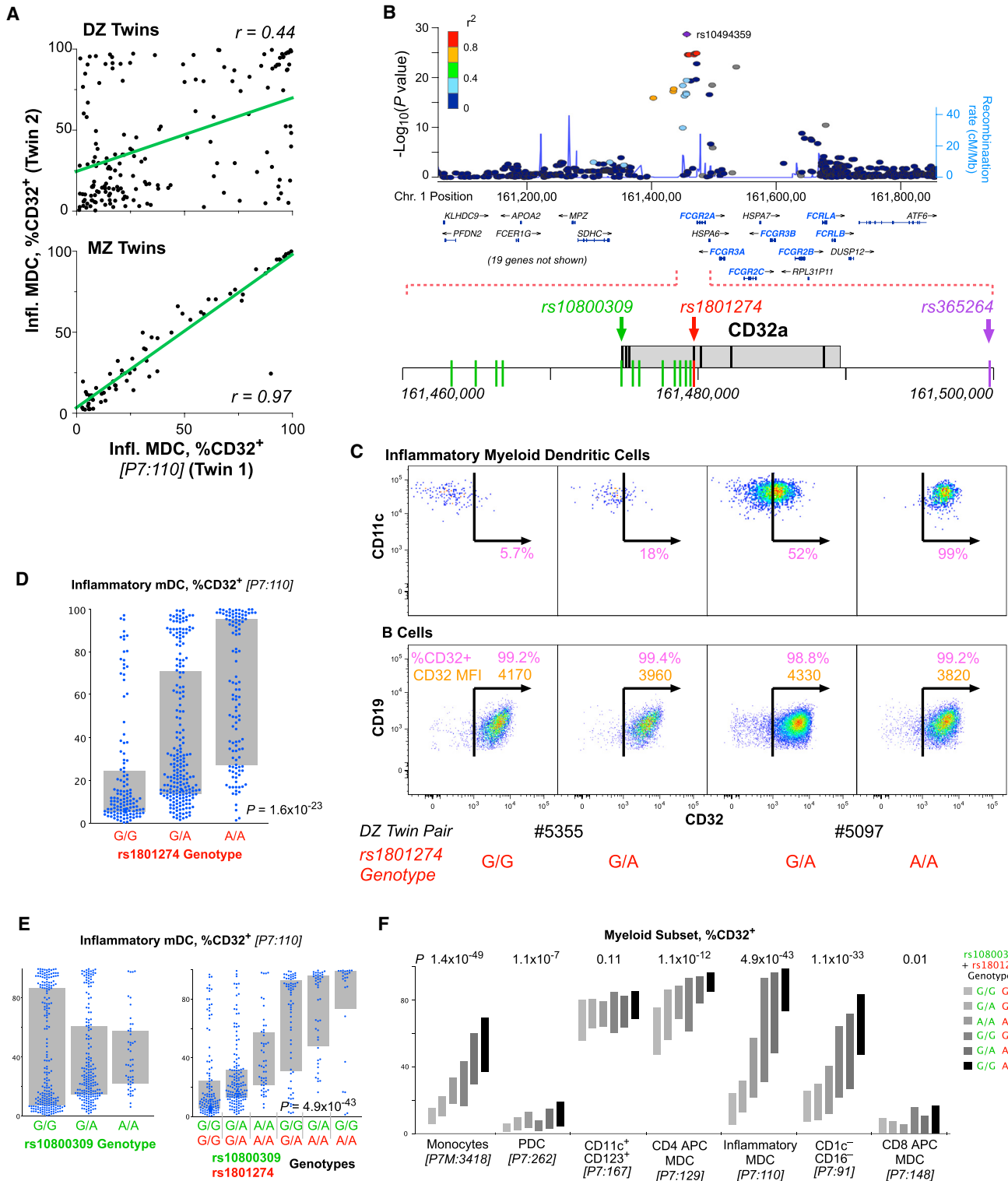


**Figure 4. Genetic Associations of the FcR Locus with Myeloid Immunophenotypes**  
 (A) The correlation of the fraction of iMDCs that are CD32<sup>+</sup> for dizygotic twins (top) and monozygotic twins (bottom). The linear correlation,  $r$ , is shown for each comparison.

(legend continued on next page)

gene controls several phenotypic features of CD39<sup>+</sup> T<sub>REG</sub>. Although we confirm an apparent association of this gene locus with the frequency of circulating CD39<sup>+</sup> T<sub>REG</sub> (Orrù et al., 2013), we show here that this is a consequence solely of altered phenotype. Quantitative analysis of CD39 protein expression on the cell surface demonstrates that the genetics of control of CD39<sup>+</sup> T<sub>REG</sub> is exerted at the level of surface protein expression, rather than cell frequency (homeostasis). This establishes a paradigm for future studies of immune traits and points to the necessity of including both cell frequency and cell protein expression analyses in immunogenetic studies of the human immune system. We also describe the association of a genetic locus containing the ecto-5'-nucleotidase (*NT5E* and *CD73*) gene with a population of CD73<sup>+</sup> T<sub>REG</sub>. From a functional perspective, it is of interest that both *CD73* and *CD39* are ectonucleotidases involved in the generation of immunosuppressive adenosine that alters T cell and NK cell activities (Deaglio et al., 2007). Thus, it appears that the *CD39* and *CD73* adenosine immunosuppressive pathway has been under evolutionary selection and might therefore be a critical determinant of functional T<sub>REG</sub> activity (Bastid et al., 2013) and establishment of tissue homeostasis. Importantly, we conclude that there is no genetic control of the frequency of T<sub>REG</sub> (i.e., CD127<sup>+</sup>CD25<sup>+</sup> memory CD4 cells), but rather, control is evinced at the level of their specific phenotype and presumably function. Furthermore, the lack of a known disease association with this locus calls into question the importance of *CD39* expression for T<sub>REG</sub> function.

We discovered several genetic associations with immune traits relevant to lymphocyte lineage and differentiation. A genetic locus containing the cell-surface death receptor *FAS* (*CD95*) was associated with the frequency of circulating T stem cell memory cells (T<sub>SCM</sub>). T<sub>SCM</sub> are a recently described infrequent and functionally important lymphocyte subset (Gattinoni et al., 2011); these cells have a largely naive T cell phenotype but are able to self-renew while displaying functional attributes of memory cells. Genetic control at the level of *CD95* suggests a potential role of *CD95* in the control of T stem cell homeostasis for not only differentiation stages such as T<sub>SCM</sub> but total CD8 as well (Figure 3). It further provides a possible link between human autoimmune syndromes based on genetic *CD95* deficiency (Strasser et al., 2009) and T<sub>SCM</sub>.

A genetic locus within a cluster of genes referred to as the “NK complex” containing *NKG2D* (*CD314* and *KLRK1*) was associated with the frequency of a distinct population of CD314<sup>-</sup>CD335<sup>+</sup> “early” (CD56<sup>+</sup>CD16<sup>-</sup>) NK cells. The *NKG2D* gene encodes for a C-type lectin protein preferentially expressed in NK cells. It binds to a diverse family of stress-induced ligands

that include MHC class I chain-related A and B proteins (*MICA* and *MICB*), essential for the activation of T cells and NK cells (Raulet et al., 2013). These data establish an unexpected link between the genetic control of the frequency of a specific subset of NK cells and a gene locus containing major genes with functional relevance to NK cell activity and their activation by stressed normal tissue cells or tumor cells.

One locus in chromosome 1q23 containing *FCGR2A*, *FCGR2B*, and *FCRLA* was associated with multiple immune traits. FcGR genes encode immunoglobulin Fc surface receptors found on macrophages, dendritic cells, and neutrophils, as well as B and NK cells, and are involved in the regulation of B cell antibody production and phagocytosis of immune complexes. The main associated immune traits were the frequencies of CD32<sup>+</sup> inflammatory dendritic cells and monocytes, as well as several T cell phenotypes. Genetic variation in the FcGR gene locus is associated with an increase in susceptibility to several autoimmune and infectious disease, including SLE, ankylosing spondylitis, HIV progression, and several other syndromes. Given the profound impact of this gene locus on particular immune cell subsets, altered function of CD32<sup>+</sup> dendritic cells could be key to increased susceptibility to these autoimmune and infectious diseases.

Indeed, our demonstration of an association between the *FCGR2A* SNP and T cell phenotypes and/or inflammatory myeloid cells (e.g., imDCs) provides a potential link between this locus and autoimmune diseases with T cell etiology. This coding SNP results in variants of the Fc receptor that have different avidities for immunoglobulin and C-reactive protein; consequently, much current research is aimed at understanding the possible functional role of these alleles in autoimmunity. However, our data suggest a different possibility with a more proximal mechanistic link: that association is with a promoter/enhancer SNP (in strong linkage disequilibrium with the coding *FCGR2A* SNP) that modulates expression of the negative regulatory CD32b molecule on imDC, monocytes, and/or T cells.

In addition to the wide range of diseases associated with the FcRG locus, further examples include a SNP within a genetic locus associated with Behçet’s disease (Kirino et al., 2013) that is in tight linkage disequilibrium with a SNP controlling the frequency of CD314<sup>-</sup>CD335<sup>+</sup> early NK cells. We also report that a genetic locus containing *FAS* and associated with Juvenile idiopathic arthritis (Hinks et al., 2013) is also associated with functionally important CD8<sup>+</sup> T stem memory cells.

These findings illustrate a key value of our database and approach: the identification of candidate immune traits associated with genetic loci of relevance to autoimmunity and infection. In summary, using one of the most comprehensive immune

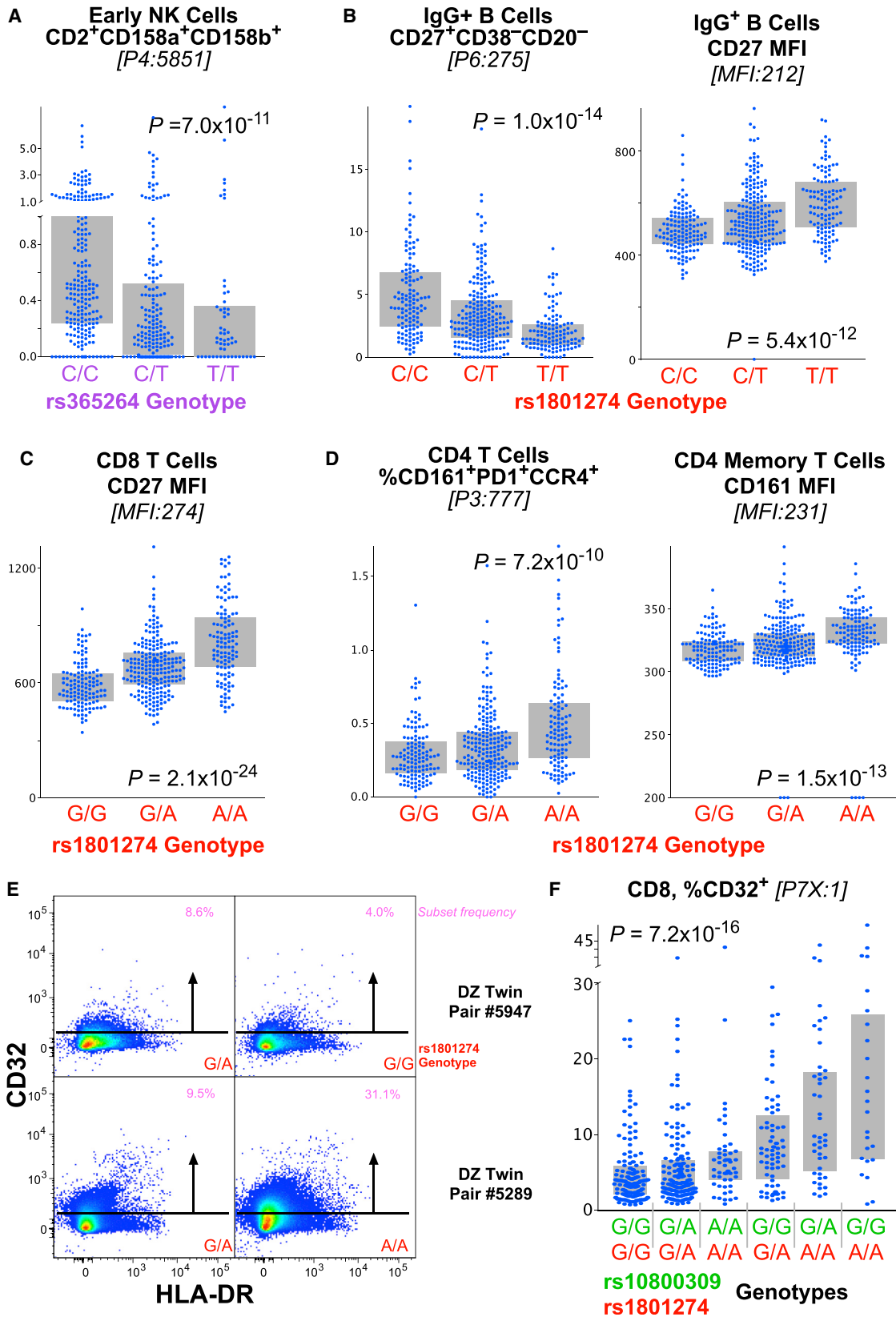
(B) Organization of the FcR locus of chromosome 1 showing the position of immunologically relevant genes. The positions of three SNPs are highlighted in color; rs1801274 and rs10800309 are the two that are most closely associated to susceptibility to SLE. SNPs shown in green were in complete linkage disequilibrium within the samples analyzed in our cohort.

(C) Sample expression profiles of CD32 on imDCs (top) and B cells (bottom). Shown are the fraction of cells that are CD32<sup>+</sup> (in pink) and, for the B cells, the CD32 SPEL (in orange). Two pairs of dizygotic twins discordant for the genotype at rs1801274 are shown.

(D) The distribution of expression of CD32<sup>+</sup> imDCs is shown by genotype at rs1801274.

(E) The expression of CD32 on the imDCs is not significantly associated with the genotype at rs10800309 by standard ANOVA ( $p = ns$ ); however, the distributions are clearly different by genotype. The combination of the genotype at rs10800309 and rs1801274 provides a dramatic distinction for the expression of CD32 on imDC.

(F) The expression profile of CD32 on seven different myeloid populations is shown, broken down by the combined genotype of the two SNPs. Bars indicate interquartile range.



(legend on next page)

phenotyping efforts to date, we identified numerous genetic loci controlling key parameters of a normal human immune system. This comprehensive human immune phenotyping bioresource will allow the identification of critical immune phenotypes associated with common autoimmune and infectious diseases, ultimately leading to accelerated discovery of mechanisms of disease and response to therapy.

## EXPERIMENTAL PROCEDURES

### Samples

This study was approved by the NIAID (NIH) IRB and London-Westminster NHS Research Ethics Committee; all participants provided informed consent. The discovery stage comprised 497 female participants from the UK Adult Twin Register, TwinsUK, with full genotyping data on 460 subjects. The TwinsUK cohort is described in detail in (Moayyeri et al., 2012). Briefly, TwinsUK is a large cohort of twins historically developed to study the heritability and genetics of diseases with a higher prevalence among women. The study population is not enriched for any particular disease or trait and is representative of the British general population of Caucasian ethnicity. Selected twins were all female with an age range of 41–77 (mean 61.4), and by self-report, 100% Caucasian with most being UK ancestry. From the subsequent genotype data, we excluded a few individuals showing evidence of non-European ancestry as assessed by principal component analysis comparison with HapMap3.

The replication stage included a further unrelated 172 TwinsUK participants with whole-genome genotyping data on 169. The samples for the discovery samples were selected to match the characteristics (age and gender) of the discovery data set. For this reason, the replication cohort included only Caucasian women with an age range of 32–83 (mean 58.2). All subjects were nominally healthy at the time of sample collection.

A total of 746 PBMC vials were analyzed: PBMC from the 669 twin specimens (plus 4 replicates) and 30 healthy controls from the US (two vials of PBMC from blood drawn six months apart were analyzed for 29 subjects, a replicate vial of PBMC from one of the two blood draws for 14 (of the 29), and one vial only for 1 subject). The samples in each stage were ordered such that twin or longitudinal control samples were analyzed in the same experimental run (each comprising 15–30 vials), whereas replicate control samples were analyzed in different experimental runs. Staining and data analyses were otherwise performed blinded to identity.

### Immunophenotyping

See [Extended Experimental Procedures](#) for cell processing details.

### Flow Cytometry and Data Analysis

Cells were analyzed in 96-well plate format on an 18-color LSR (BD Biosciences) using an HTS unit. Each run on the flow cytometer was accompanied by a set of compensation controls of antibody-stained IgG kappa beads (BD Biosciences). Data were evaluated on FlowJo software v9.7 (FlowJo, LLC). Post-processing of data and visualizations were done with JMP v10 (SAS) and SPICE v5.3 (NIAID; Roederer et al., 2011).

### Gating

A graphic depicting the fluorescence distribution of all samples in the discovery cohort is shown in [Figure S1](#). [Figures S2](#) and [S3](#) illustrate the gating hierarchy for a single sample. The [Extended Experimental Procedures](#) describe the generation of the ~80,000 gates analyzed.

For the discovery cohort, there were 20 experimental runs for 543 samples (501 twin specimens from 497 subjects and 42 US control specimens from 14 subjects). Within each run, uniform scatter gating was used. Each sample was gated on time (to eliminate spurious events from beginning or end of sample run); this gate could vary by sample. With two major exceptions, all samples received the same fluorescence gating. After the third run, we chose to replace the CD4 reagent in panels 1, 2, and 5 due to poor performance; this necessitated a different CD4 gating for those samples. Similarly, the reagents in the “dump” channel of panel 7 were modified after 6 runs.

For the replication cohort, there were 8 experimental runs for 203 samples (172 twin specimens from 172 subjects and 31 US control specimens from 16 subjects). All analysis procedures were identical to the discovery cohort. Minor modifications to the panels were necessitated by unavailability of the same lots of reagents, but these did not impact enumeration of subsets. Specimen processing for the replication cohort was initiated after final analysis of the discovery cohort.

### Genotyping

Genotyping was conducted with a combination of Illumina arrays (HumanHap300 and HumanHap610Q) (Richards et al., 2008; Soranzo et al., 2009). The Illuminus calling algorithm (Teo et al., 2007) was used to assign genotypes. No calls were assigned if an individual's most likely genotype was called with less than a posterior probability threshold of 0.95. Validation of pooling was achieved via a visual inspection of 100 random, shared SNPs for overt batch effects. Finally, intensity cluster plots of significant SNPs were visually inspected for over-dispersion, biased no calling, and/or erroneous genotype assignment. SNPs exhibiting any of these characteristics were discarded. Stringent QC measures were performed on the genotypes prior to data analysis. The sample exclusion criteria were: (1) sample call rate < 98%, (2) heterozygosity across all SNPs  $\geq 2$  SD from the sample mean; (3) evidence of non-European ancestry as assessed by principle component analysis comparison with HapMap3 populations; (4) observed pairwise identity by descent (IBD) probabilities suggestive of sample identity errors; (5) misclassified monozygotic and dizygotic twins were corrected based on IBD probabilities. The exclusion criteria for SNPs were: (1) Hardy-Weinberg equilibrium (HWE)  $p$  value <  $10^{-6}$ , assessed in a set of unrelated samples; (2) minor allele frequency (MAF) < 1%, assessed in a set of unrelated samples; (3) SNP call rate < 97% (SNPs with MAF  $\geq 5\%$ ) or < 99% (for  $1\% \leq \text{MAF} < 5\%$ ). Alleles of both data sets from the genotyping arrays were aligned to HapMap2 or HapMap3 forward strand alleles. Imputation was performed using the IMPUTE v2 software package (Howie et al., 2009). After imputation of the 2,986,407 SNPs available for analysis, 1,419,558 SNPs passed further QC (call rate  $\geq 95\%$ , MAF  $\geq 0.05$ , HWE  $\geq 10^{-4}$ ) and were used for analysis.

### Statistical Analyses

#### Selection of Subsets for Heritability and GWAS Analysis

Full details are in the [Extended Experimental Procedures](#). In brief, we eliminated CSFs with frequencies below 0.1% or above 99% ([Figure S4A](#)). From these, we selected ~200 for in-depth analysis based on heritability or description in the literature (“canonical”).

#### Genome-wide Association Analysis

Because of relatedness in the TwinsUK cohort, we utilized the GenABEL software package (Aulchenko et al., 2007), which is designed for GWAS analysis of family-based data by incorporating pairwise kinship matrix calculated using

## Figure 5. Genetic Associations of the FcR Locus with Lymphoid Immunophenotypes

- (A) The genotype of rs365264 (close to CD16a on chromosome 1) is strongly associated CD56<sup>+</sup>CD16<sup>-</sup> (“early”) NK cells that are CD2<sup>+</sup>CD158a<sup>+</sup>CD158b<sup>+</sup>.  
 (B) The genotype of rs1801274 is associated with the frequency of memory IgG<sup>+</sup> B cells that are CD27<sup>+</sup>CD38<sup>-</sup>CD20<sup>-</sup> as well as the fraction of CD27<sup>+</sup> cells. Note that, for this case, a lower frequency of the subset (left) is associated with higher protein expression (right).  
 (C) Similarly, the genotype of rs1801274 is strongly associated with the cell-surface expression of CD27 on CD8 T cells.  
 (D) The genotype of rs1801274 is strongly associated with the cell-surface expression of CD161 on CD4 T cells, as well as CD4 T cells that are CD161<sup>+</sup>PD1<sup>+</sup>CCR4<sup>+</sup>.  
 (E) CD8 T cells express low levels of CD32 depending on genotype as shown by flow cytometry.  
 (F) The fraction of CD8 T cells that express CD32 is strongly associated with the rs10800309:rs1801274 diplotype (see [Figure 4](#)).  
 Bars indicate interquartile ranges.

**Table 2. Overlapping Associations with Complex Diseases**

Immune Trait Association						Disease Association			
Gene (Chr)	Marker	Trait ID	Trait Phenotype	Beta	p Value	Reported SNP	Disease	Best P	Reference
<i>FCGR2A</i> (1)	rs1801274	P7:110	iMDC: %CD32 <sup>+</sup>	0.2	1.6E−23	rs1801274 (A)	IBD	2.1E−38	(Jostins et al., 2012)
		MFI:189	CD27 on IgA <sup>+</sup> B	0.13	6.5E−11		Kawasaki disease	7.4E−11	(Khor et al., 2011)
		MFI:212	CD27 on IgG <sup>+</sup> B	0.14	5.4E−12		ulcerative colitis	2.2E−20	(Anderson et al., 2011)
		MFI:231	CD161 on CD4 T	0.13	2.6E−11		ankylosing-spondylitis	1.4E−09	(Cortes et al., 2013)
		MFI:504	CD27 on CD4 T	0.15	5.4E−14		SLE	6.8E−07	(Harley et al., 2008)
		MFI:552	CD27 on CD8 T	0.19	1.3E−21		HIV progression	1.0E−04*	(Forthal et al., 2007)
		P7:224	CD1c <sup>+</sup> mDC: %CD32	0.12	4.4E−09		lymphoma	0.006*	(Wang et al., 2006)
						malaria	0.013*	(Sinha et al., 2008)	
<i>FCGR2A</i> (1)	rs10494359	P7:110	iMDC: %CD32 <sup>+</sup>	0.34	2.5E−29	rs10494360 (r <sup>2</sup> = 0.94)	rheumatoid arthritis	9.3E−05*	(Eyre et al., 2012)
<i>ZNF804A</i> (2)	rs6755404	P2:3367	Effector CD4: CD127 <sup>−</sup> PD1 <sup>−</sup>	0.09	3.8E−04	rs6755404 (A)	malaria	1.2E−06	(Band et al., 2013)
<i>MIR216B</i> (2)	rs6751715	P3:5372	CD8 T: %CXCR3 <sup>−</sup> R4 <sup>+</sup> R6 <sup>+</sup> R10 <sup>−</sup>	−0.09	1.5E−05	rs6751715	HIV	1.1E−06	(Fellay et al., 2009)
		P3:5661	CD8 T: %CD161 <sup>+</sup>	−0.07	5.1E−04				
		P6:197	IgA <sup>+</sup> B: %CD27 <sup>−</sup> CD38 <sup>−</sup>	0.07	7.0E−04				
		P3:5658	CD8 T: %CD161 <sup>+</sup> PD1 <sup>−</sup>	−0.07	7.8E−04				
<i>LOC100505836</i> (3)	rs2593321	Lin:19	%NKT	0.08	5.5E−04	rs2593321	HIV-1 control	7.7E−06	(Pelak et al., 2010)
<i>MICA</i> (6)	rs4418214	P6:112	IgE <sup>+</sup> B: %CD20 <sup>−</sup> CD27 <sup>−</sup> CD38 <sup>+</sup>	0.12	7.6E−04	rs4418214 (C)	HIV-1 control	1.4E−34	(Pereyra et al., 2010)
<i>BTNL2</i> (6)	rs3817963	P2:12609	CD8 T: %CD25 <sup>+</sup> CD38 <sup>+</sup> 45RO <sup>+</sup>	−0.08	3.5E−04	rs3817963 (A)	hepatitis C liver cirrhosis	1.3E−08	(Urabe et al., 2013)
		P2:10486	CD8 T: %CD25 <sup>+</sup> CD38 <sup>+</sup>	−0.08	4.1E−04				(Urabe et al., 2013)
<i>HLA-DQB1</i> (6)	rs2856718	P2:12609	CD8 T: %CD25 <sup>+</sup> CD38 <sup>+</sup> 45RO <sup>+</sup>	−0.08	5.3E−04	rs2856718 (A)	hepatitis B	4.0E−37	(Mbarek et al., 2011)
		P2:10486	CD8 T: %CD25 <sup>+</sup> CD38 <sup>+</sup>	−0.07	7.8E−04				
<i>EHMT2</i> (6)	rs652888	MFI:578	CD3 on CD8 T	−0.08	5.7E−04	rs652888	chronic hepatitis B	7.1E−13	(Kim et al., 2013)
<i>MTCO3P1 - HLA-DQA2</i> (62)	rs4273729	P2:10486	CD8 T: %CD25 <sup>+</sup> CD38 <sup>+</sup>	0.08	1.4E−04	rs4273729	chronic hepatitis C	1.7E−16	(Duggal et al., 2013)
		P2:12609	CD8 T: %CD25 <sup>+</sup> CD38 <sup>+</sup> 45RO <sup>+</sup>	0.08	2.3E−04				
<i>ADGB</i> (6)	rs2275606	P1:12906	CD8 T: %TSCM	0.13	6.3E−04	rs2275606 (A)	leprosy	3.9E−14	(Zhang et al., 2011)
<i>ABO</i> (9)	rs8176722	MFI:1	CD123 on mDC	−0.14	1.4E−04	rs8176722 (A)	malaria	8.9E−10	(Band et al., 2013)
<i>ACTA2, FAS</i> (10)	rs7069750	P1:6601	CD8 T: %TSCM	−0.14	4.1E−12	rs7069750 (C)	juvenile idiopathic arthritis	2.9E−08	(Hinks et al., 2013)
						rs2147420 (r <sup>2</sup> = 1)	CLL	3.1E−13	(Berndt et al., 2013)
<i>KLRC4-KLRK1</i> (12)	rs1049172	P4:3551	NK: %CD314 <sup>−</sup> CD158a <sup>+</sup>	−0.13	8.8E−09	rs2617170 (r <sup>2</sup> = 0.922)	Behçet's disease	1.3E−09	(Kirino et al., 2013)
		P4:4832	NK: %CD314 <sup>−</sup> CCR7 <sup>−</sup>	−0.23	7.6E−22				
		P4:5538	NK: %CD314 <sup>−</sup> CD335 <sup>+</sup>	−0.27	1.4E−30				
<i>MMP16</i> (8)	rs160441	P4:3551	NK: %CD314 <sup>−</sup> CD158a <sup>+</sup>	−0.08	2.3E−05	rs160441	tuberculosis	8.4E−06	(Thye et al., 2010)
<i>ARHGAP20</i> (11)	rs1469170	P4:3551	NK: %CD314 <sup>−</sup> CD158a <sup>+</sup>	−0.08	5.6E−04	rs1469170 (A)	malaria	8.0E−08	(Band et al., 2013)

Association results from the discovery cohort immune trait analyses are reported in the first six columns. The trait ID is fully described in Table S2. The disease-associated variant, pathology, the disease-associated SNP's best-reported p value are indicated in the 7<sup>th</sup>–9<sup>th</sup> columns, respectively. The risk alleles presented correlate with increased disease susceptibility and the r<sup>2</sup> between disease SNP and immune trait, if different, are reported in parentheses after the reported SNP. \*Disease association is significant with candidate SNP method/gene approach.

genotyping data in the polygenic model to correct relatedness and hidden population stratification. The score test implemented in the software was used to test the association between a given SNP and the trait. Additional quality control was conducted on the association results: minor allele frequency (MAF) > 0.1, Hardy-Weinberg equilibrium <  $10^{-8}$ , SNP call rate > 90%. For our results, we used a genome-wide significance threshold of  $p < 3.3 \times 10^{-10}$ . This threshold represents a standard genome-wide significance threshold ( $p < 5 \times 10^{-8}$ ) further adjusted for 151 independent tests (the number of traits analyzed for GWAS in the discovery cohort). Because there is a high intercorrelation among some of the 151 analyzed traits, this is a very conservative approach and ensures the robustness of our findings. Genome-wide validations were also performed on normalized residuals (after corrections for age), with GenABEL taking into account family structure in the model. The validation p value threshold was set to  $p < 0.05$ .

Results from the genome-wide analyses of all the analyzed traits for both the discovery and the replication cohorts were meta-analyzed. Fixed effects inverse-variance weighted meta-analyses were conducted using METAL (Willer et al., 2010), with significance evaluated at  $p < 5 \times 10^{-8}$ .

Finally, correlation against the FCRG “diplotype” shown in Figures 4 and S8 was done using JMP; ANOVA p values without correction for family structure are reported.

#### Identifying Traits Correlated with SNPs

Once we had identified significant associations between the selected 151 traits and all SNPs based on standard analyses, we looked for pleiotropic effects of those SNPs. Approximately 1,200 SNPs from about 18 unlinked loci were correlated against all traits.

To correct for multiple comparisons, we evaluated the covariance among all traits. As shown in Figure S4B, there are less than 1,800 traits that show a covariance less than 0.7. Thus, Bonferroni correction sets a significance threshold of  $p < 2.8 \times 10^{-5}$ . In our analyses, which covered about 20 unlinked loci, we used a more conservative threshold, requiring a Wilcoxon rank association of trait values with SNP genotype to be significant if  $p < 10^{-7}$ .

#### GWAS Catalog Look-Ups

In order to ascertain whether the variants from the associations of the immune cell subsets analyses overlapped with significant disease associations, the GWAS catalog (<http://www.genome.gov/gwastudies/>), Immunobase (<http://immunobase.org/page/Welcome/display>), and SNPedia (<http://www.snpedia.com>) repositories were used. Gene regions and variants reaching genome-wide significance were searched on these repositories and overlapping associations or correlations with proxy SNPs or those in strong LD are reported in Table 2.

#### BioData Repository

Raw and summary data are available for downloading and analysis. Genotype data are available upon request to the authors. See [Extended Experimental Procedures](#) for detailed downloading instructions.

#### SUPPLEMENTAL INFORMATION

Supplemental Information includes Extended Experimental Procedures, eight figures, and six tables and can be found with this article online at <http://dx.doi.org/10.1016/j.cell.2015.02.046>.

#### AUTHOR CONTRIBUTIONS

M.R., T.D.S., and F.O.N. designed and supervised the study; I.T., L.N., M.T.B., and F.V. processed samples, which were coordinated by P.D.M.; M.H.B., Y.M., P.C., and P.D.M. performed experimental work; M.R., L.Q., M.M., and M.H.B. performed primary data analysis; M.R., L.Q., M.M., and C.M. performed statistical analyses; and M.R., L.Q., M.M., P.D.M., T.D.S., and F.O.N. wrote the manuscript.

#### ACKNOWLEDGMENTS

This work was supported by the Vaccine Research Center (NIAID, NIH) intramural research program and by the Department of Health via the National Insti-

tute for Health Research (NIHR) comprehensive Biomedical Research Centre award to Guy's & St. Thomas' NHS Foundation Trust in partnership with King's College London, King's College Hospital NHS Foundation (guysbrc-2012-1) Trust, and Dunhill Medical Trust. TwinsUK is also supported by the Wellcome Trust, and TDS is an ERC Advanced Researcher. We wish to thank Kaime Song, Steve Peretto, Richard Nguyen, Lynda Myles, Gabriela Surdulescu, Dylan Hodgkiss, and Ayrin Nessa for technical help with the samples, as well as the TwinsUK volunteers for participation.

Received: October 9, 2014

Revised: December 22, 2014

Accepted: February 4, 2015

Published: March 12, 2015

#### REFERENCES

- Ahmadi, K.R., Hall, M.A., Norman, P., Vaughan, R.W., Snieder, H., Spector, T.D., and Lanchbury, J.S. (2001). Genetic determinism in the relationship between human CD4+ and CD8+ T lymphocyte populations? *Genes Immun.* 2, 381–387.
- Amadori, A., Zamarchi, R., De Silvestro, G., Forza, G., Cavatton, G., Danieli, G.A., Clementi, M., and Chieco-Bianchi, L. (1995). Genetic control of the CD4/CD8 T-cell ratio in humans. *Nat. Med.* 1, 1279–1283.
- Anderson, C.A., Boucher, G., Lees, C.W., Franke, A., D'Amato, M., Taylor, K.D., Lee, J.C., Goyette, P., Imielinski, M., Latiano, A., et al. (2011). Meta-analysis identifies 29 additional ulcerative colitis risk loci, increasing the number of confirmed associations to 47. *Nat. Genet.* 43, 246–252.
- Antonoli, L., Pacher, P., Vizi, E.S., and Haskó, G. (2013). CD39 and CD73 in immunity and inflammation. *Trends Mol. Med.* 19, 355–367.
- Aulchenko, Y.S., Ripke, S., Isaacs, A., and van Duijn, C.M. (2007). GenABEL: an R library for genome-wide association analysis. *Bioinformatics* 23, 1294–1296.
- Band, G., Le, Q.S., Jostins, L., Pirinen, M., Kivinen, K., Jallow, M., Sisay-Joof, F., Bojang, K., Pinder, M., Sirugo, G., et al.; Malaria Genomic Epidemiology Network (2013). Imputation-based meta-analysis of severe malaria in three African populations. *PLoS Genet.* 9, e1003509.
- Bastid, J., Cottalorda-Regairaz, A., Alberici, G., Bonnefoy, N., Eliaou, J.F., and Bensussan, A. (2013). ENTPD1/CD39 is a promising therapeutic target in oncology. *Oncogene* 32, 1743–1751.
- Berndt, S.I., Skibola, C.F., Joseph, V., Camp, N.J., Nieters, A., Wang, Z., Cozen, W., Monnereau, A., Wang, S.S., Kelly, R.S., et al. (2013). Genome-wide association study identifies multiple risk loci for chronic lymphocytic leukemia. *Nat. Genet.* 45, 868–876.
- Borsellino, G., Kleiweietfeld, M., Di Mitri, D., Sternjak, A., Diamantini, A., Gionetto, R., Hopner, S., Centonze, D., Bernardi, G., Dell'Acqua, M.L., et al. (2007). Expression of ectonucleotidase CD39 by Foxp3+ Treg cells: hydrolysis of extracellular ATP and immune suppression. *Blood* 110, 1225–1232.
- Casanova, J.L., and Abel, L. (2004). The human model: a genetic dissection of immunity to infection in natural conditions. *Nat. Rev. Immunol.* 4, 55–66.
- Clementi, M., Forabosco, P., Amadori, A., Zamarchi, R., De Silvestro, G., Di Gianantonio, E., Chieco-Bianchi, L., and Tenconi, R. (1999). CD4 and CD8 T lymphocyte inheritance. Evidence for major autosomal recessive genes. *Hum. Genet.* 105, 337–342.
- Cortes, A., Hadler, J., Pointon, J.P., Robinson, P.C., Karaderi, T., Leo, P., Cremin, K., Pryce, K., Harris, J., Lee, S., et al.; International Genetics of Ankylosing Spondylitis Consortium (IGAS); Australo-Anglo-American Spondyloarthritis Consortium (TASC); Groupe Française d'Etude Génétique des Spondylarthrites (GFEGS); Nord-Trøndelag Health Study (HUNT); Spondyloarthritis Research Consortium of Canada (SPARCC); Wellcome Trust Case Control Consortium 2 (WTCCC2) (2013). Identification of multiple risk variants for ankylosing spondylitis through high-density genotyping of immune-related loci. *Nat. Genet.* 45, 730–738.
- Cotsapas, C., and Hafler, D.A. (2013). Immune-mediated disease genetics: the shared basis of pathogenesis. *Trends Immunol.* 34, 22–26.

- Damoiseaux, J.G., Cautain, B., Bernard, I., Mas, M., van Breda Vriesman, P.J., Druet, P., Fournié, G., and Saoudi, A. (1999). A dominant role for the thymus and MHC genes in determining the peripheral CD4/CD8 T cell ratio in the rat. *J. Immunol.* *163*, 2983–2989.
- Deaglio, S., Dwyer, K.M., Gao, W., Friedman, D., Usheva, A., Erat, A., Chen, J.F., Enjyoji, K., Linden, J., Oukka, M., et al. (2007). Adenosine generation catalyzed by CD39 and CD73 expressed on regulatory T cells mediates immune suppression. *J. Exp. Med.* *204*, 1257–1265.
- Duggal, P., Thio, C.L., Wojcik, G.L., Goedert, J.J., Mangia, A., Latanich, R., Kim, A.Y., Lauer, G.M., Chung, R.T., Peters, M.G., et al. (2013). Genome-wide association study of spontaneous resolution of hepatitis C virus infection: data from multiple cohorts. *Ann. Intern. Med.* *158*, 235–245.
- Evans, D.M., Frazer, I.H., and Martin, N.G. (1999). Genetic and environmental causes of variation in basal levels of blood cells. *Twin Res.* *2*, 250–257.
- Eyre, S., Bowes, J., Diogo, D., Lee, A., Barton, A., Martin, P., Zernakova, A., Stahl, E., Viatte, S., McAllister, K., et al.; Biologics in Rheumatoid Arthritis Genetics and Genomics Study Syndicate; Wellcome Trust Case Control Consortium (2012). High-density genetic mapping identifies new susceptibility loci for rheumatoid arthritis. *Nat. Genet.* *44*, 1336–1340.
- Fellay, J., Ge, D., Shianna, K.V., Colombo, S., Ledergerber, B., Cirulli, E.T., Urban, T.J., Zhang, K., Gumbs, C.E., Smith, J.P., et al.; NIAID Center for HIV/AIDS Vaccine Immunology (CHAVI) (2009). Common genetic variation and the control of HIV-1 in humans. *PLoS Genet.* *5*, e1000791.
- Ferreira, M.A., Mangino, M., Brumme, C.J., Zhao, Z.Z., Medland, S.E., Wright, M.J., Nyholt, D.R., Gordon, S., Campbell, M., McEvoy, B.P., et al.; International HIV Controllers Study (2010). Quantitative trait loci for CD4:CD8 lymphocyte ratio are associated with risk of type 1 diabetes and HIV-1 immune control. *Am. J. Hum. Genet.* *86*, 88–92.
- Forthal, D.N., Landucci, G., Bream, J., Jacobson, L.P., Phan, T.B., and Montoya, B. (2007). FcγRIIIa genotype predicts progression of HIV infection. *J. Immunol.* *179*, 7916–7923.
- Gattinoni, L., Lugli, E., Ji, Y., Pos, Z., Paulos, C.M., Quigley, M.F., Almeida, J.R., Gostick, E., Yu, Z., Carpenito, C., et al. (2011). A human memory T cell subset with stem cell-like properties. *Nat. Med.* *17*, 1290–1297.
- Hall, M.A., Ahmadi, K.R., Norman, P., Snieder, H., MacGregor, A.J., Vaughan, R.W., Spector, T.D., and Lanchbury, J.S. (2000). Genetic influence on peripheral blood T lymphocyte levels. *Genes Immun.* *1*, 423–427.
- Harley, J.B., Alarcón-Riquelme, M.E., Criswell, L.A., Jacob, C.O., Kimberly, R.P., Moser, K.L., Tsao, B.P., Vyse, T.J., Langefeld, C.D., Nath, S.K., et al.; International Consortium for Systemic Lupus Erythematosus Genetics (SLEGEN) (2008). Genome-wide association scan in women with systemic lupus erythematosus identifies susceptibility variants in ITGAM, PXX, KIAA1542 and other loci. *Nat. Genet.* *40*, 204–210.
- Hinks, A., Cobb, J., Marion, M.C., Prahalad, S., Sudman, M., Bowes, J., Martin, P., Comeau, M.E., Sajuthi, S., Andrews, R., et al.; Boston Children's JIA Registry; British Society of Paediatric and Adolescent Rheumatology (BSPAR) Study Group; Childhood Arthritis Prospective Study (CAPS); Childhood Arthritis Response to Medication Study (CHARMS); German Society for Pediatric Rheumatology (GKJR); JIA Gene Expression Study; NIAMS JIA Genetic Registry; TREAT Study; United Kingdom Juvenile Idiopathic Arthritis Genetics Consortium (UKJIAGC) (2013). Dense genotyping of immune-related disease regions identifies 14 new susceptibility loci for juvenile idiopathic arthritis. *Nat. Genet.* *45*, 664–669.
- Howie, B.N., Donnelly, P., and Marchini, J. (2009). A flexible and accurate genotype imputation method for the next generation of genome-wide association studies. *PLoS Genet.* *5*, e1000529.
- Jostins, L., Ripke, S., Weersma, R.K., Duerr, R.H., McGovern, D.P., Hui, K.Y., Lee, J.C., Schumm, L.P., Sharma, Y., Anderson, C.A., et al.; International IBD Genetics Consortium (IBDGC) (2012). Host-microbe interactions have shaped the genetic architecture of inflammatory bowel disease. *Nature* *491*, 119–124.
- Khor, C.C., Davila, S., Breunis, W.B., Lee, Y.C., Shimizu, C., Wright, V.J., Yeung, R.S., Tan, D.E., Sim, K.S., Wang, J.J., et al.; Hong Kong–Shanghai Kawasaki Disease Genetics Consortium; Korean Kawasaki Disease Genetics Consortium; Taiwan Kawasaki Disease Genetics Consortium; International Kawasaki Disease Genetics Consortium; US Kawasaki Disease Genetics Consortium; Blue Mountains Eye Study (2011). Genome-wide association study identifies FCGR2A as a susceptibility locus for Kawasaki disease. *Nat. Genet.* *43*, 1241–1246.
- Kim, Y.J., Kim, H.Y., Lee, J.H., Yu, S.J., Yoon, J.H., Lee, H.S., Kim, C.Y., Cheong, J.Y., Cho, S.W., Park, N.H., et al. (2013). A genome-wide association study identified new variants associated with the risk of chronic hepatitis B. *Hum. Mol. Genet.* *22*, 4233–4238.
- Kirino, Y., Bertsias, G., Ishigatsubo, Y., Mizuki, N., Tugal-Tutkun, I., Seyahi, E., Ozyazgan, Y., Sacli, F.S., Erer, B., Inoko, H., et al. (2013). Genome-wide association analysis identifies new susceptibility loci for Behçet's disease and epistasis between HLA-B\*51 and ERAP1. *Nat. Genet.* *45*, 202–207.
- Kraal, G., Weissman, I.L., and Butcher, E.C. (1983). Genetic control of T-cell subset representation in inbred mice. *Immunogenetics* *18*, 585–592.
- Kyvic, K. (2000). Generalisability and assumptions of twin studies. In *Advances in Twin and Sib-Pair Analysis*, T.D. Spector, H. Sneider, and A.J. MacGregor, eds. (London: Greenwich Medical Media), pp. 67–77.
- Lugli, E., Dominguez, M.H., Gattinoni, L., Chattopadhyay, P.K., Bolton, D.L., Song, K., Klatt, N.R., Brenchley, J.M., Vaccari, M., Gostick, E., et al. (2013). Superior T memory stem cell persistence supports long-lived T cell memory. *J. Clin. Invest.* *123*, 594–599.
- Mahnke, Y.D., Beddall, M.H., and Roederer, M. (2012). OMP-013: differentiation of human T-cells. *Cytometry A* *81*, 935–936.
- Mahnke, Y.D., Beddall, M.H., and Roederer, M. (2013a). OMP-015: human regulatory and activated T-cells without intracellular staining. *Cytometry A* *83*, 179–181.
- Mahnke, Y.D., Beddall, M.H., and Roederer, M. (2013b). OMP-017: human CD4(+) helper T-cell subsets including follicular helper cells. *Cytometry A* *83*, 439–440.
- Mahnke, Y.D., Beddall, M.H., and Roederer, M. (2013c). OMP-019: quantification of human  $\gamma\delta$ T-cells, iNKT-cells, and hematopoietic precursors. *Cytometry A* *83*, 676–678.
- Mbarek, H., Ochi, H., Urabe, Y., Kumar, V., Kubo, M., Hosono, N., Takahashi, A., Kamatani, Y., Miki, D., Abe, H., et al. (2011). A genome-wide association study of chronic hepatitis B identified novel risk locus in a Japanese population. *Hum. Mol. Genet.* *20*, 3884–3892.
- Moayyeri, A., Hammond, C.J., Hart, D.J., and Spector, T.D. (2012). Effects of age on genetic influence on bone loss over 17 years in women: the Healthy Ageing Twin Study (HATS). *J. Bone Miner. Res.* *27*, 2170–2178.
- Nalls, M.A., Couper, D.J., Tanaka, T., van Rooij, F.J., Chen, M.H., Smith, A.V., Toniolo, D., Zaki, N.A., Yang, Q., Greinacher, A., et al. (2011). Multiple loci are associated with white blood cell phenotypes. *PLoS Genet.* *7*, e1002113.
- Neale, M., and Cardon, L. (1992). *Methodology for Genetic Studies of Twins and Families* (Dordrecht: Kluwer Academic Publishers).
- Okada, Y., Hirota, T., Kamatani, Y., Takahashi, A., Ohmiya, H., Kumasaka, N., Higasa, K., Yamaguchi-Kabata, Y., Hosono, N., Nalls, M.A., et al. (2011). Identification of nine novel loci associated with white blood cell subtypes in a Japanese population. *PLoS Genet.* *7*, e1002067.
- Orrù, V., Steri, M., Sole, G., Sidore, C., Virdis, F., Dei, M., Lai, S., Zoledziwska, M., Busonero, F., Mulas, A., et al. (2013). Genetic variants regulating immune cell levels in health and disease. *Cell* *155*, 242–256.
- Parkes, M., Cortes, A., van Heel, D.A., and Brown, M.A. (2013). Genetic insights into common pathways and complex relationships among immune-mediated diseases. *Nat. Rev. Genet.* *14*, 661–673.
- Pelak, K., Goldstein, D.B., Walley, N.M., Fellay, J., Ge, D., Shianna, K.V., Gumbs, C., Gao, X., Maia, J.M., Cronin, K.D., et al.; Infectious Disease Clinical Research Program HIV Working Group; National Institute of Allergy and Infectious Diseases Center for HIV/AIDS Vaccine Immunology (CHAVI) (2010). Host determinants of HIV-1 control in African Americans. *J. Infect. Dis.* *201*, 1141–1149.
- Pereyra, F., Jia, X., McLaren, P.J., Telenti, A., de Bakker, P.I., Walker, B.D., Ripke, S., Brumme, C.J., Pulit, S.L., Carrington, M., et al. (2010). The major

- genetic determinants of HIV-1 control affect HLA class I peptide presentation. *Science* 330, 1551–1557.
- Raj, T., Rothamel, K., Mostafavi, S., Ye, C., Lee, M.N., Replogle, J.M., Feng, T., Lee, M., Asinovsky, N., Frohlich, I., et al. (2014). Polarization of the effects of autoimmune and neurodegenerative risk alleles in leukocytes. *Science* 344, 519–523.
- Raulet, D.H., Gasser, S., Gowen, B.G., Deng, W., and Jung, H. (2013). Regulation of ligands for the NKG2D activating receptor. *Annu. Rev. Immunol.* 31, 413–441.
- Richards, J.B., Rivadeneira, F., Inouye, M., Pastinen, T.M., Soranzo, N., Wilson, S.G., Andrew, T., Falchi, M., Gwilliam, R., Ahmadi, K.R., et al. (2008). Bone mineral density, osteoporosis, and osteoporotic fractures: a genome-wide association study. *Lancet* 371, 1505–1512.
- Roederer, M., Nozzi, J.L., and Nason, M.C. (2011). SPICE: exploration and analysis of post-cytometric complex multivariate datasets. *Cytometry A* 79, 167–174.
- Sakaguchi, S., Miyara, M., Costantino, C.M., and Hafler, D.A. (2010). FOXP3+ regulatory T cells in the human immune system. *Nat. Rev. Immunol.* 10, 490–500.
- Sinha, S., Mishra, S.K., Sharma, S., Patibandla, P.K., Mallick, P.K., Sharma, S.K., Mohanty, S., Pati, S.S., Mishra, S.K., Ramteke, B.K., et al.; Indian Genome Variation Consortium (2008). Polymorphisms of TNF-enhancer and gene for FcγRIIIa correlate with the severity of falciparum malaria in the ethnically diverse Indian population. *Malar. J.* 7, 13.
- Soranzo, N., Rivadeneira, F., Chinappan-Horsley, U., Malkina, I., Richards, J.B., Hammond, N., Stolk, L., Nica, A., Inouye, M., Hofman, A., et al. (2009). Meta-analysis of genome-wide scans for human adult stature identifies novel Loci and associations with measures of skeletal frame size. *PLoS Genet.* 5, e1000445.
- Starbeck-Miller, G.R., Badovinac, V.P., Barber, D.L., and Harty, J.T. (2014). Cutting edge: Expression of FcγRIIB tempers memory CD8 T cell function in vivo. *J. Immunol.* 192, 35–39.
- Strasser, A., Jost, P.J., and Nagata, S. (2009). The many roles of FAS receptor signaling in the immune system. *Immunity* 30, 180–192.
- Teo, Y.Y., Inouye, M., Small, K.S., Gwilliam, R., Deloukas, P., Kwiatkowski, D.P., and Clark, T.G. (2007). A genotype calling algorithm for the Illumina BeadArray platform. *Bioinformatics* 23, 2741–2746.
- Thye, T., Vannberg, F.O., Wong, S.H., Owusu-Dabo, E., Osei, I., Gyapong, J., Sirugo, G., Sisay-Joof, F., Enimil, A., Chinbuah, M.A., et al.; African TB Genetics Consortium; Wellcome Trust Case Control Consortium (2010). Genome-wide association analyses identifies a susceptibility locus for tuberculosis on chromosome 18q11.2. *Nat. Genet.* 42, 739–741.
- Urabe, Y., Ochi, H., Kato, N., Kumar, V., Takahashi, A., Muroyama, R., Hosono, N., Otsuka, M., Tateishi, R., Lo, P.H., et al. (2013). A genome-wide association study of HCV-induced liver cirrhosis in the Japanese population identifies novel susceptibility loci at the MHC region. *J. Hepatol.* 58, 875–882.
- van Dongen, J., Slagboom, P.E., Draisma, H.H., Martin, N.G., and Boomsma, D.I. (2012). The continuing value of twin studies in the omics era. *Nat. Rev. Genet.* 13, 640–653.
- Wang, S.S., Cerhan, J.R., Hartge, P., Davis, S., Cozen, W., Severson, R.K., Chatterjee, N., Yeager, M., Chanock, S.J., and Rothman, N. (2006). Common genetic variants in proinflammatory and other immunoregulatory genes and risk for non-Hodgkin lymphoma. *Cancer Res.* 66, 9771–9780.
- Willer, C.J., Li, Y., and Abecasis, G.R. (2010). METAL: fast and efficient meta-analysis of genomewide association scans. *Bioinformatics* 26, 2190–2191.
- Zhang, F., Liu, H., Chen, S., Low, H., Sun, L., Cui, Y., Chu, T., Li, Y., Fu, X., Yu, Y., et al. (2011). Identification of two new loci at IL23R and RAB32 that influence susceptibility to leprosy. *Nat. Genet.* 43, 1247–1251.

## EXTENDED EXPERIMENTAL PROCEDURES

### Immunophenotyping

#### **PBMC Isolation, Cryopreservation, and Staining**

PBMCs from the twin cohort were purified by blood centrifugation on a density gradient (Lymphoprep, PAA, Pasching, Austria). Cells were viably frozen in RPMI 1640 (Life Technologies, Carlsbad, CA) supplemented with 11.25% HSA (Gemini Bio-Products, West Sacramento, CA)/10% DMSO (Sigma St. Louis, MO) and stored in liquid nitrogen until further use. Healthy control samples were drawn at the NIH and also viably frozen using a similar protocol. Twin cohort samples were shipped in liquid nitrogen to the NIH laboratories and processed in bulk.

#### **Cell Processing**

Cryopreserved vials of PBMCs were thawed in a 37°C water bath for 1 min and resuspended in 10 ml of RPMI supplemented with 10% heat-inactivated newborn calf serum (Life Technologies), and 0.5 U/ml Benzamide (EMD Biosciences), pre-warmed to room temperature. Tubes were centrifuged for 10 min at 700 x g in a tabletop Sorval centrifuge. After removal of the supernatant, cells were resuspended in 10 ml of the RPMI supplemented as above, warmed to 37°C and centrifuged for 3 min at 860 x g. PBMCs were resuspended in 1 ml PBS (Life Technologies) and 10  $\mu$ l were removed to a 96 well plate (Corning) containing a 10  $\mu$ l solution of ethidium bromide/acridine orange (EB/AO) (Life Technologies) for counting on a Nexcelom Cellometer. Cells were washed at 860 x g for 3 min and resuspended in 730  $\mu$ l of PBS. 100  $\mu$ l was transferred to each of 5 wells of a 96 well plate for room temperature staining and each of 2 wells of another 96 well plate for 37°C staining (see [Table S1](#) for temperatures by Panel). The plates were centrifuged at 860 x g for 3 min and the PBS removed by aspiration.

#### **Reagents**

See [Table S1](#) for a list of reagents used in each of the seven panels. Immunofluorescence reagents were purchased from Becton Dickinson, BioLegend, eBiosciences, Life Technologies, Beckman Coulter, Fisher Scientific, or Miltenyi Biotec; or conjugated in house. All reagents were titrated at the staining temperature used for any given panel. A full description of the optimization of some panels is published: Panel P1 ([Mahnke et al., 2012](#)), P2 ([Mahnke et al., 2013a](#)), P3 ([Mahnke et al., 2013b](#)) and P5 ([Mahnke et al., 2013c](#)).

#### **Staining**

Each well was resuspended in 50  $\mu$ l containing an Aqua Blue (Life Technologies) solution of a 1:39 stock (in water) diluted 1: 20 in PBS. For staining of monocytes and dendritic cells the Aqua Blue was supplemented with Fc blocking reagent at 2.5  $\mu$ l (Miltenyi). Plates were incubated for 15 min in the dark then centrifuged at 860 x g for 3 min. Supernatant was removed by aspiration. Master mixes were prepared for each panel in staining buffer (RPMI without phenol red (Life Technologies) supplemented with 4% heat-inactivated fetal calf serum) and centrifuged at 12,000 x g for 10 min (Eppendorf centrifuge 5415D) in order to remove aggregates. Cell pellets were resuspended in 50  $\mu$ l of the panel antibodies and incubated for 40 min at room temperature or 37°C. All wells were washed, as above, 3 times with staining buffer and resuspended in 250  $\mu$ l of PBS containing 1% paraformaldehyde (Tousimis Research Corporation Inc.).

#### **Gating**

A graphic depicting the fluorescence distribution of all samples in the discovery cohort is shown in [Figure S1](#). [Figures S2](#) and [S3](#) illustrate the gating hierarchy for a single sample. As illustrated in these graphics (and also [Figure S1](#)), we generated a large number of subsets for analysis that encompassed all combinations of certain markers. For each panel, we first identified major “lineages” or parent subsets. For example, in Panels 1 and 2, these include CD4 T cells, CD8 T cells, double negative (CD4<sup>+</sup>CD8<sup>-</sup>) T cells, and double positive (CD4<sup>+</sup>CD8<sup>+</sup>) T cells. In Panel 3, the parent subsets included naive or memory CD4 or CD8 T cells. Within each parent subset, we then created Boolean combination gates for the set of markers that exhibited heterogeneous expression patterns within the parent subsets. In addition, we computed the median fluorescence intensity (MFI) for all markers of the parent subsets. MFIs were only computed for cells positive for a given marker, so that the frequency of the positive cells did not influence the MFI. For example, the CD27 MFI on CD4 T cells was computed as the median expression of CD27 on CD4<sup>+</sup>CD27<sup>+</sup> T cells. In the manuscript, we refer to the MFI calculation as estimating the relative “surface protein expression level” (SPEL).

FlowJo was used to export MFI values, as well as cell subset frequencies (CSF) for all Boolean combination gates. These gates comprise non-overlapping populations. For example, a Boolean combination of three markers “A,” “B,” and “C” leads to 8 subsets, including A<sup>+</sup>B<sup>+</sup>C<sup>+</sup>, A<sup>+</sup>B<sup>+</sup>C<sup>-</sup>, A<sup>+</sup>B<sup>-</sup>C<sup>+</sup>, etc. Automated scripts in JMP further processed these data to generate all possible combinations that ignored one or more markers. For example, A<sup>+</sup>B<sup>+</sup> (also denoted as A<sup>+</sup>B<sup>+</sup>C<sup>0</sup>) was computed as the sum of A<sup>+</sup>B<sup>+</sup>C<sup>+</sup> and A<sup>+</sup>B<sup>+</sup>C<sup>-</sup>; A<sup>+</sup>B<sup>-</sup> (also denoted as A<sup>+</sup>B<sup>-</sup>C<sup>0</sup>) as the sum of A<sup>+</sup>B<sup>-</sup>C<sup>+</sup> and A<sup>+</sup>B<sup>-</sup>C<sup>-</sup>; A<sup>+</sup> (also denoted as A<sup>+</sup>B<sup>0</sup>C<sup>0</sup>) was computed as the sum all four combinations of B and C with A<sup>+</sup>. Thus, this step creates all combinations of positive, negative, or ignored (“0”) for all markers, which we refer to as “tri-boolean” combination gates. Given “n” markers, there are 2<sup>n</sup> Boolean gates and 3<sup>n</sup> tri-boolean gates. Every tri-boolean gate was assigned a unique identifier, given as “Panel number:Serial number.” Thus, P1:336 is a unique subset from Panel 1. The serial numbers have no meaning other than to distinguish gating used to define the subsets.

Note that any given cell belongs to only one Boolean gate, but belongs to multiple tri-boolean gates. Thus, there is considerable covariation of tri-boolean frequencies. For the seven immunophenotyping panels, we created over 4,000 boolean subsets, resulting in nearly 80,000 tri-boolean subsets. The combination of tri-boolean subset frequencies and MFI values comprise the 78,683 traits we analyzed.

## Statistical Analyses

### Selection of Subsets for Heritability and GWAS Analysis

For genome-wide association analysis, we selected a subset of traits. First, we eliminated those CSFs whose mean frequency (within their parent “lineage”) was below 0.1% or above 99%. As shown in [Figure S4A](#), this reduced the number of traits to below 50,000. From these, we selected approximately 200 for in-depth analysis as follows.

First, we chose 97 functionally-distinct subsets based on our experience as well as definitions in the literature. These included differentiation stages of T cells (naive, stem cell memory, central, transitional, effector and terminal effector memory) and B cells (immature, mature, etc.); lineages of CD4 T cells (Th1, Th2, Th17, Th22), and so forth. These are referred to as “canonical” subsets.

Next, we roughly estimated heritability for all traits based on Falconer’s formula based on the difference between the intra-class correlation coefficients of the two zygositys (i.e.,  $h^2 = 2 \times [r_{MZ} - r_{DZ}]$ ). Of the 97 pre-defined canonical subsets, 46 showed no evidence of heritability nor were of sufficient interest biologically and were not included in further genetic analysis. From the global trait list, we then selected 100 highly-heritable, independent traits across all seven panels, choosing from highly related subsets the one with the simplest definition (for example, if all of  $A^+$ ,  $A^+B^+$ , and  $A^+B^-$  were highly heritable, we chose only  $A^+$ ). These 100 traits, together with 51 canonical traits, were then submitted for GWAS analysis.

We then estimated heritability of the 151 traits using structural equation modeling (SEM) to separate the observed phenotypic variance into three latent sources of variation: additive genetic variance (A), shared/common environmental variance (C), and non-shared/unique environmental variance (E) (Neale and Cardon, 1992). Additive genetic influences are indicated when monozygotic (MZ) twins are more similar than dizygotic (DZ) twins. The common environmental component estimates the contribution of family environment which is assumed to be equal in both MZ and DZ twin pairs (Kyvic, 2000), whereas the unique environmental component does not contribute to twin similarity, rather it estimates the effects that apply only to each individual and includes measurement error. Any greater similarity between MZ twins than DZ twins is attributed to greater sharing of genetic influences. Heritability is defined as the proportion of the phenotypic variation attributable to genetic factors, and using SEM is given by the equation,  $h^2 = (A)/(A + C + E)$ .

The heritability analysis was estimated on the inverse normalized trait values. Each trait was adjusted for age by linear regression after removing the outliers ( $> 4$  standard deviations). The residuals were then normalized using inverse normal transformation and used for both the heritability and genome wide association analysis.

### BioData Repository

Raw and summary data is available for downloading and analysis. Genotype data is available upon request to the authors.

### Flow Cytometry Data

FCS data files are deposited in the International Society for the Advancement of Cytometry public data repository. This includes 130 GB of data, comprising  $> 5,200$  individual data files. In addition, the FlowJo workspaces used to analyze these files are also available, providing the complete gating scheme, statistical analysis, and graphical analysis for every single data file. These files are available at <http://www.tinyurl.com/twinsFACSdata>.

### GWAS Summary

The detailed summary of all GWAS analyses performed on the 150 selected traits is provided; each trait is a separate file. These files can be downloaded from <ftp://twinnr-ftp.kcl.ac.uk/ImmuneCellScience>, in folder “2-GWASResults.”

### Demographics

Anonymized demographic information (anonymized unique family ID, age, twin type) for subjects is provided in a single file, <ftp://twinnr-ftp.kcl.ac.uk/ImmuneCellScience>, file name “3-Demographics.zip.”

### Heritability

Estimated heritability (Falconer’s) for all 78,000 traits, including a detailed definition of each of the traits, suitable for sorting and analysis is available in a single file. This file can be downloaded from <ftp://twinnr-ftp.kcl.ac.uk/ImmuneCellScience>, file name “4-Trait Analysis.zip.”

### Trait Values

Every measured trait value is in a single file, containing a table of 78,000 values for each individual. This file can be downloaded from <ftp://twinnr-ftp.kcl.ac.uk/ImmuneCellScience>, file name “5-Trait Values.zip.”

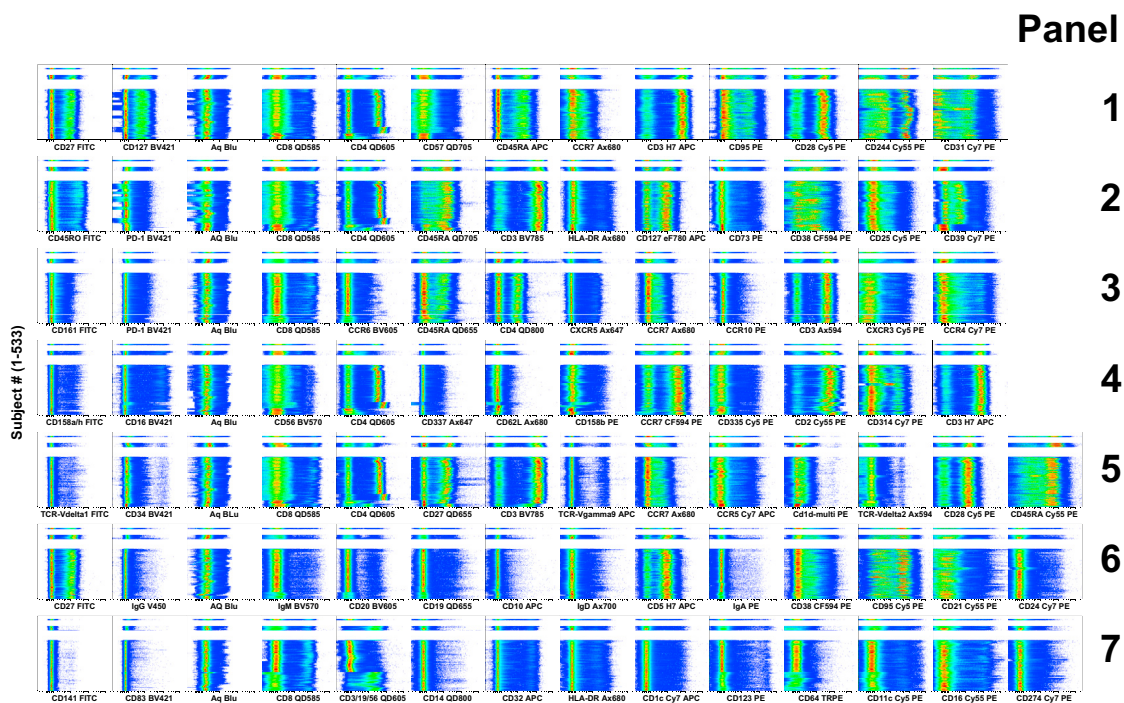


**Figure S1. Fluorescence Distribution of All Immunophenotyping Panels for All Subjects, Related to Experimental Procedures**

For each of the seven panels, 1000 events from each data file for each of the 543 samples analyzed for the discovery cohort were merged into a single file. Each of the fluorescent markers used in the panel (abscissa) are shown in separate graphics, plotted against all subjects (ordinate). Clusters of rows constitute a single run encompassing 10 to 30 separate subjects. After three runs, the panels were modified slightly to incorporate a different CD4 reagent after 3 runs, and a different “dump” reagents after 7 runs, but otherwise were identical across the entire cohort.

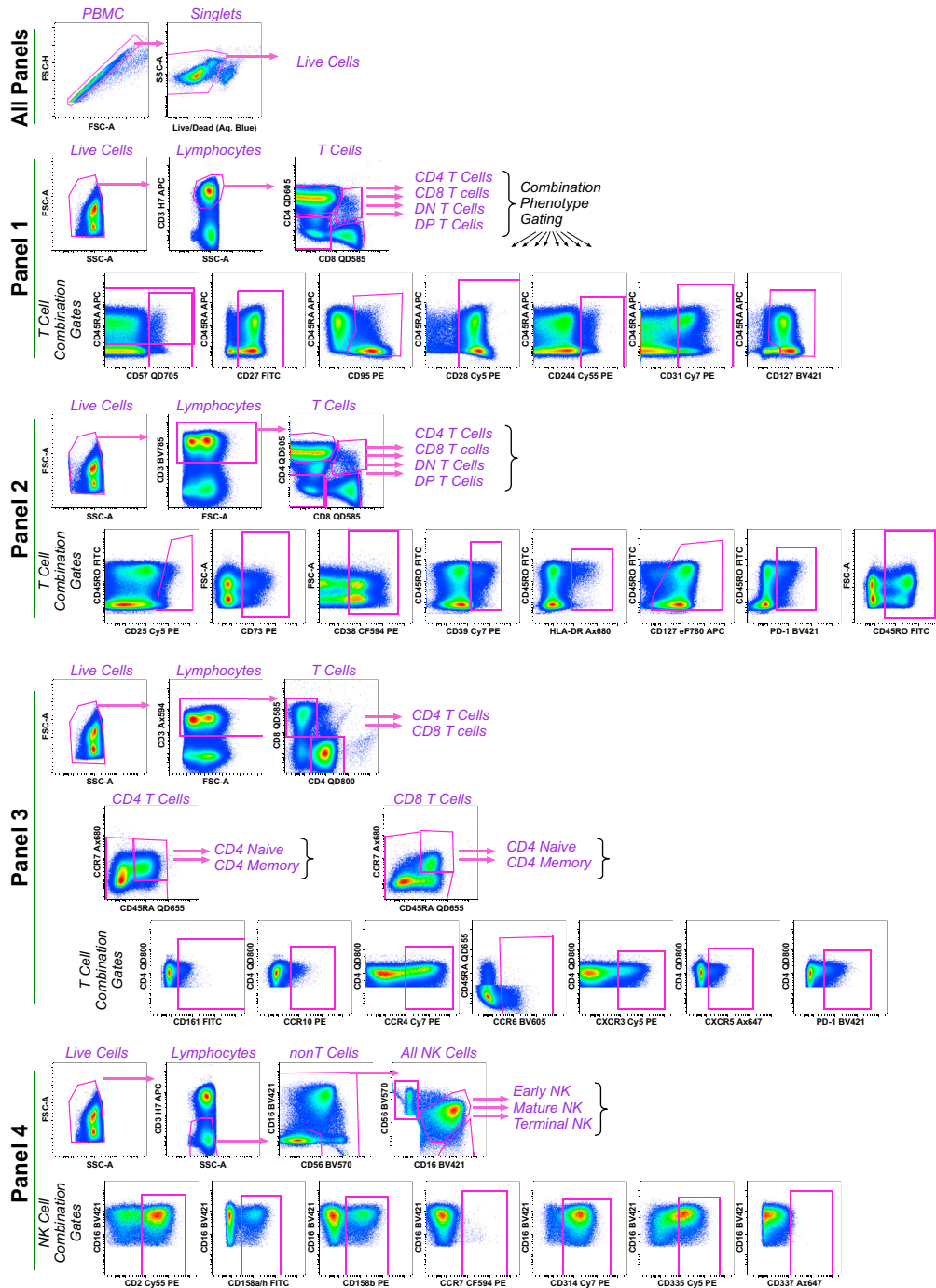


**Figure S2. Gating Hierarchy to Identify Subsets within PBMC for Immunophenotyping Panels 1 through 4, Related to Experimental Procedures**

As shown in the very top row, all data files were first preprocessed to include only singlet events as well as live cells based on aqua blue staining. The remaining gating hierarchy for each of the panels is shown. The top line(s) of graphs show the gates used to identify “lineages” or “differentiation stages.” Within each lineage/stage, all combinations of the gates shown on the bottom line were applied in a Boolean fashion (e.g., in panel one, there are eight separate gates to identify the expression pattern of eight different markers; the complete combination results in 256 gates applied to each of the four “lineages”). During post-processing analysis, combinatorial analysis on these 256 Boolean combinations was done to create all  $3^8$  possible combinations of gates for each marker (i.e., positive, negative, or ignored: “tri-boolean” combination gates). Canonical names of “lineages” and “differentiation stages” are provided as a rough guide for the cell populations and are not meant to be definitive.

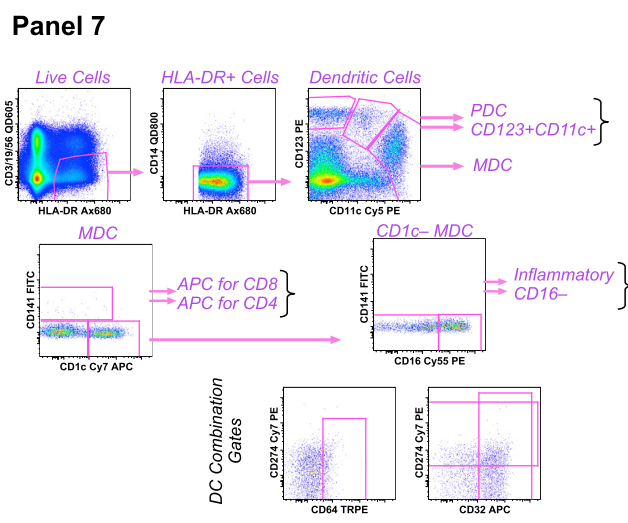
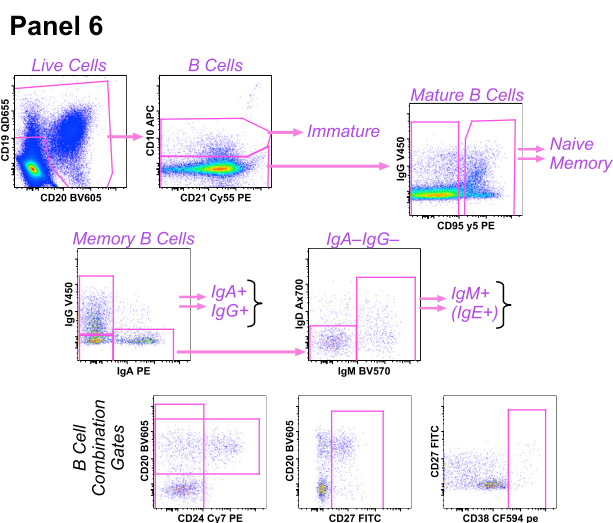
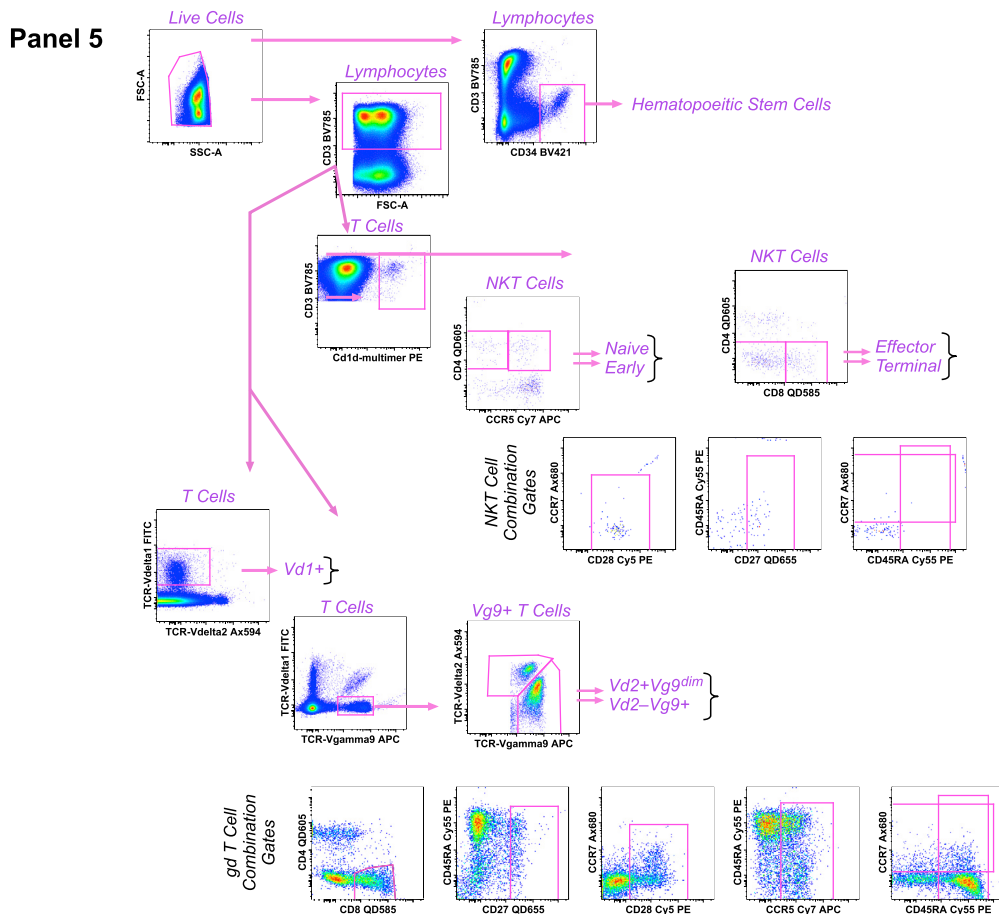


**Figure S3. Gating Hierarchy to Identify Subsets within PBMC for Immunophenotyping Panels 5 through 7, Related to Experimental Procedures**

Similar to Figure S2, cells were divided into subsets first by “lineage” gating as shown by the arrows, and then, as indicated, the combinatorial boolean gating was applied to each of these. In panel six, mature memory B cells that are negative for IgM, IgA, and IgG are likely to be reasonably pure populations of IgE expressing cells and are denoted as “(IgE).” Canonical names of “lineages” and “differentiation stages” are provided as a rough guide for the cell populations and are not meant to be definitive.

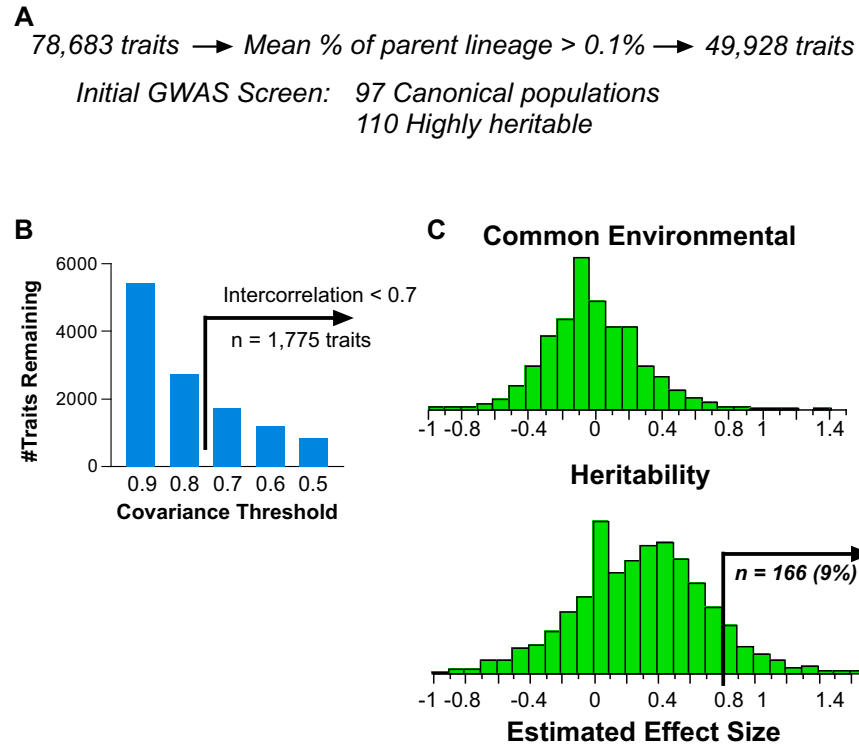


**Figure S4. Summary of the Immunophenotyping Traits Analyzed, Related to Figure 1**

(A) Of the nearly 80,000 traits (frequencies and fluorescence intensities), more than one third were eliminated from analyses as they represented subset frequencies that were too low for robust analysis (less than 0.1% of the parental “lineage” gate). For our initial GWAS analysis reported in this manuscript, we chose about 200 traits for analysis. 97 represent “canonical” populations defined in the literature (such as differentiation or activation stages); 100 were chosen from the most heritable.

(B) Of the nearly 50,000 traits, many are highly inter-correlated because they represent strongly overlapping populations of cells. To estimate degrees of freedom in the dataset, we computed how many traits remain after eliminating those that covary with another trait with a variance greater than a certain threshold. We cross-correlated all traits against all traits, and progressively eliminated those with the highest covariance. For example, eliminating traits that correlate with a variance greater than 0.9 reduces the number of independent traits from 50,000 to just over 5,000. There were nearly 1,800 traits with an intra-correlation less than 0.7.

(C) Falconer’s formula was applied to the intraclass correlations on MZ and DZ twin pairs to estimate the covariation due to common environmental factors (upper) as well as genetic heritability (lower) for the 1,775 traits with a variance less than 0.7. Of these, 9% showed estimated heritability of greater than 80%.

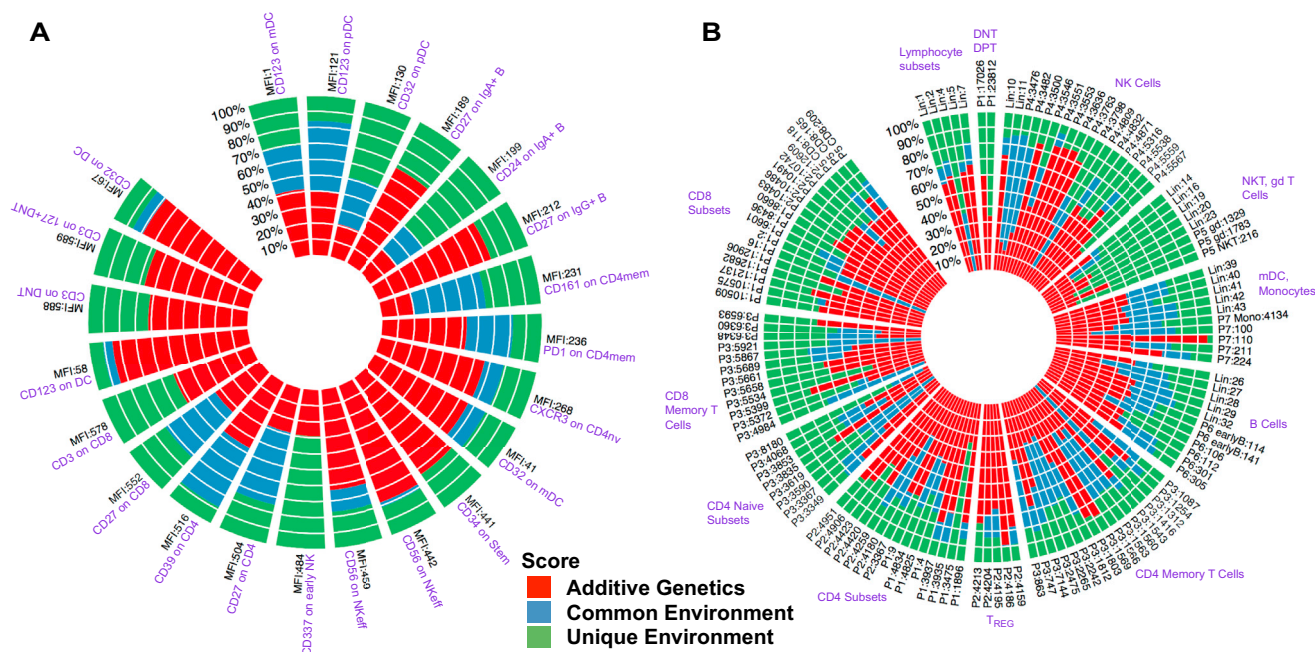


**Figure S5. Summary Heritability Plots, Related to Figure 1**

(A and B) The proportions of the additive genetics, common environment and unique environment components of the ACE twin model for heritability estimation are denoted by red, blue and green for each trait. Black trait IDs are explained in Table S2; the purple trait descriptions are approximate, broad “nicknames” for the general subset related to each group of traits.

(A) Traits related to phenotype of cells (SPELs).

(B) Traits related to representation of cell subsets (CSFs).

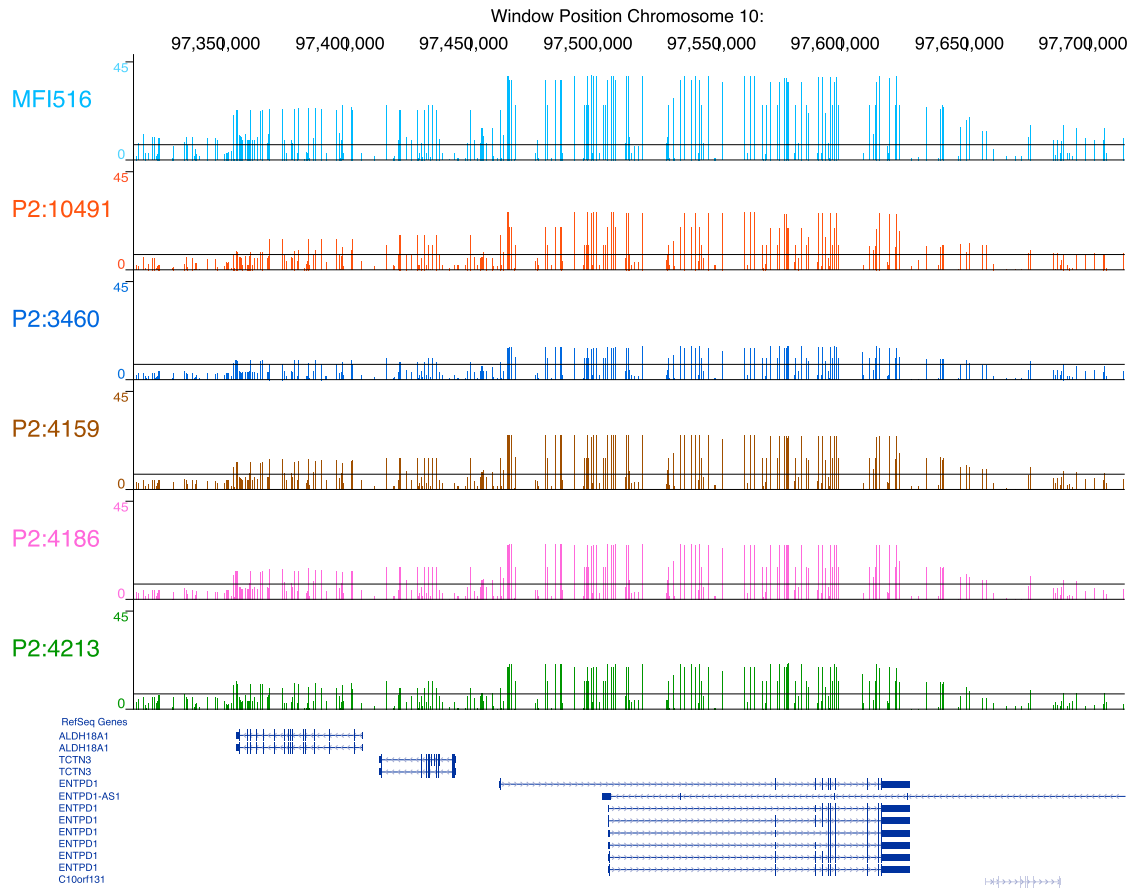


**Figure S6. LocusZoom of Chromosome 10, Related to Figure 2**  
 Regional plots of immune subsets with genome-wide associations with at the chromosome 10 *ENTPD* locus.

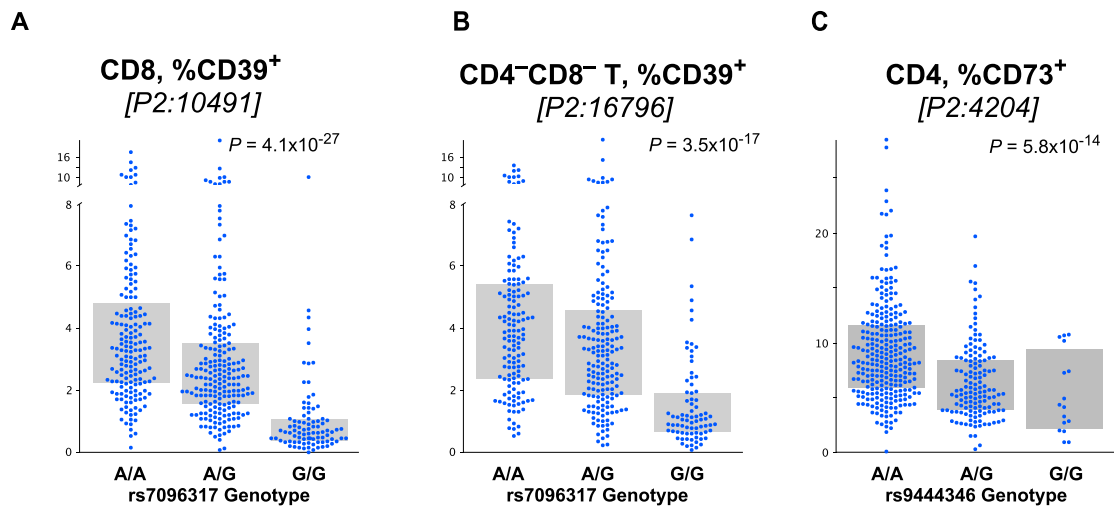


**Figure S7. Additional Genetic Associations with T<sub>REG</sub> Phenotype Cells, Related to Figure 2**

(A and B) Similar to that shown for CD4 T cells (Figure 2), the expression of CD39 on CD8 T cells and CD4<sup>-</sup>CD8<sup>+</sup> T cells, while very infrequent, is very strongly associated with the genotype of SNPs in the CD39 gene locus.

(C) The proportion of CD73<sup>+</sup> cells within CD4 T cells is significantly associated with rs9344528, located in an intron of the gene encoding CD73. Bars indicate interquartile range; ANOVA P-values are given.

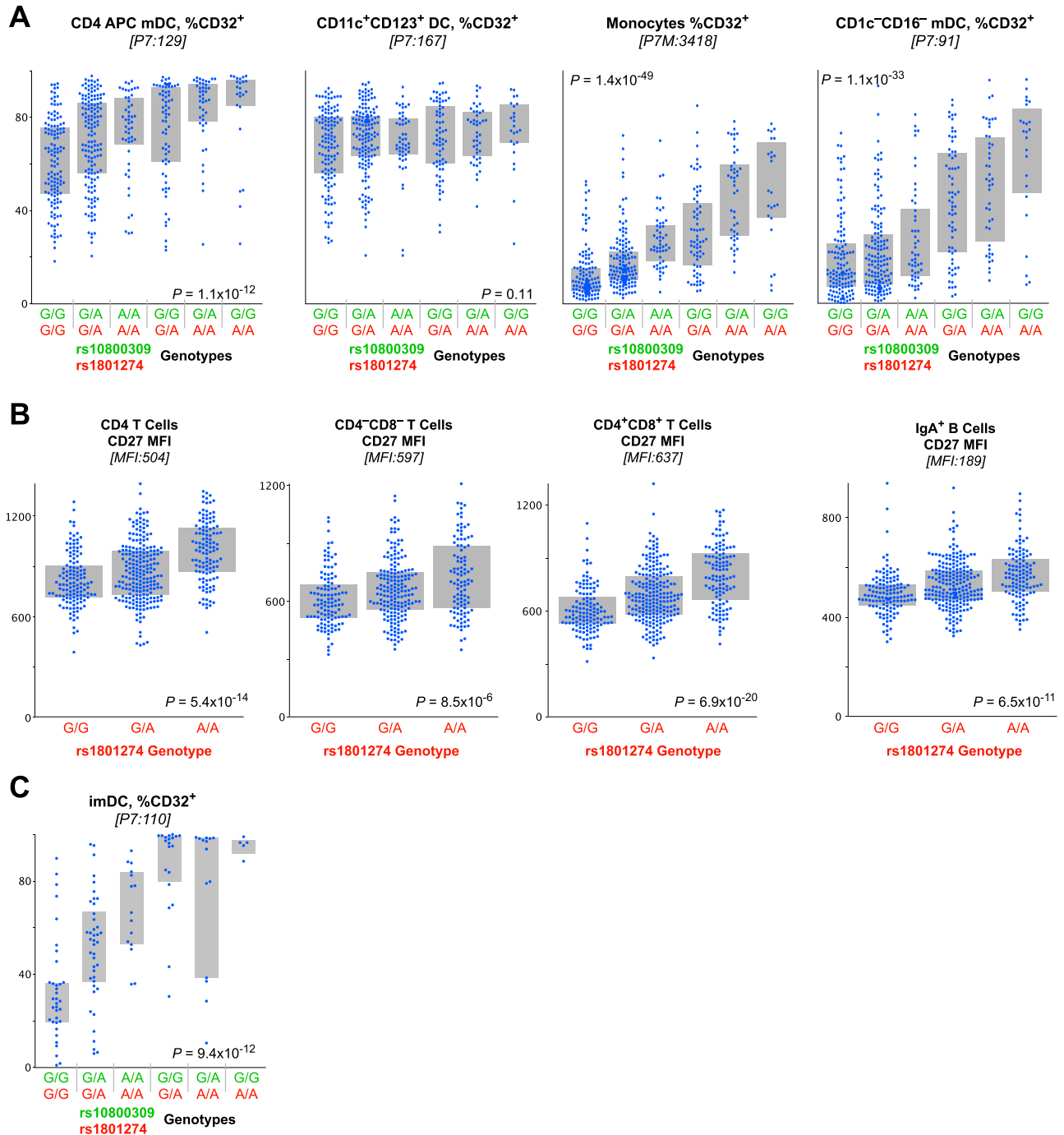


**Figure S8. Additional Genetic Associations of the FcR Locus with Immunophenotypes, Related to Figure 5**

(A) Detailed bar charts showing individual data points for the summary graphs shown in Figure 4F. Bars indicate interquartile range; ANOVA P-values are given.

(B) The genotype of rs1801274 is strongly associated with the cell surface expression of CD27 on CD4 T cells, CD4<sup>-</sup>CD8<sup>-</sup> T cells, and CD4<sup>+</sup>CD8<sup>+</sup> T cells, in a similar pattern to that seen for CD8 T cells (Figure 5). Likewise, the genotype of rs1801274 is strongly associated with the cell surface expression of CD27 on IgA<sup>+</sup> B cells, as for IgG<sup>+</sup> B cells (Figure 5).

(C) Bar chart showing association between FcR diplotype and CD32<sup>+</sup> imDC in the replication cohort (for this analysis, n = 130). Bars indicate interquartile range; ANOVA P-values is given.